

**TO STUDY THE EFFECT OF HEAT INPUT ON THE
MICROSTRUCTURE OF WELDMENT IN WELDING
OF H.S.L.A. (MICRO ALLOYED) STEEL**

A DISSERTATION

*submitted in partial fulfillment of the
requirements for the award of the degree*

of

Master of Engineering

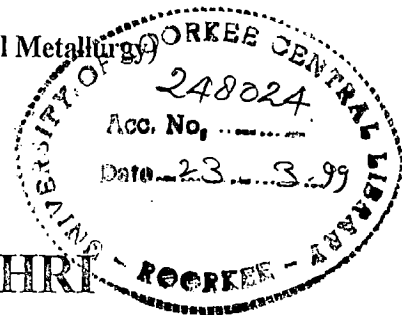
in

Metallurgical Engineering

(with specialization in Industrial Metallurgy)

By

PANKAJ JOHRI



**DEPARTMENT OF METALLURGICAL
AND MATERIALS ENGINEERING
UNIVERSITY OF ROORKEE
ROORKEE - 246 667 (INDIA)
JANUARY, 1998**

LP

CANDIDATE'S DECLARATION

I hereby declare that the work being presented in this dissertation entitled "**TO STUDY THE EFFECT OF HEAT INPUT ON THE MICROSTRUCTURE OF WELDMENT IN WELDING OF H.S.L.A. (MICRO ALLOYED) STEEL**" in partial fulfillment of the requirement for the award of the degree of **Master of Engineering in Metallurgical Engineering with Specialization in Industrial Metallurgy** of the University of Roorkee, Roorkee, is an authentic record of my own work carried out during August 1996 and then a period from September 1997 to January 1998 under the guidance of **Dr. S.K. Nath**, Reader and **Dr. G.C. Kaushal**, Associate Professor, Department of Metallurgical and Materials Engineering, University of Roorkee, Roorkee.

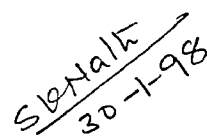
The matter presented in this dissertation has not been submitted by me for the award of any other degree or diploma.

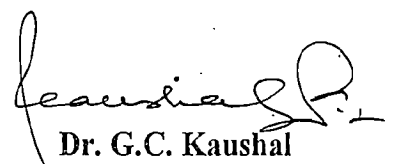
Dated : 31.1.98
Place : Roorkee


(PANKAJ JOHRI)

CERTIFICATE

This is to certify that the above statement made by the candidate is correct to the best of our knowledge.


Dr. S.K. Nath
Reader
Deptt. of Metallurgical
& Materials Engg.
University of Roorkee
Roorkee - 247 667, INDIA


Dr. G.C. Kaushal
Associate Professor
Deptt. of Metallurgical
& Materials Engg.
University of Roorkee
Roorkee - 247 667, INDIA

ACKNOWLEDGEMENT

The author wish to take this opportunity to record his indebtedness with sincere and heartfelt gratitude to **Dr. S.K. Nath**, Reader and **Dr. G.C. Kaushal**, Associate Professor, Department of Metallurgical and Materials Engineering, University of Roorkee, Roorkee for their inspiration and active supervision, through provoking discussions, criticism and suggestions given by them during the entire period of investigation. Without their timely and untiring help it would not have been possible to present this dissertation in its present form.

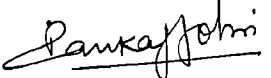
The author is grateful to all the technical staff of the Metallurgical and Materials Engineering Department, specially Mr. R.K. Sharma, Mr. S.K. Seth, Mr. Narendra Kumar (Computer Lab), Mr. B.D. Sharma, Mr. J.P. Sharma and Mr. H.K Ahuja for their cooperation extended to him during this work.

The author acknowledges the support extended to him by his parents and sister during the compilation of this work.

In the end, the author would like to extend his sincere thanks to all the near and dear ones with whose efforts and cooperation, the work could take this shape.

Roorkee

Jan. 31, 1998


(PANKAJ JOHRI)

CONTENTS

<i>Candidate's Declaration</i>	<i>i</i>
<i>Acknowledgement</i>	<i>ii</i>
<i>List of Figures</i>	<i>iii</i>
<i>List of Tables</i>	<i>iv</i>
<i>Abstract</i>	<i>v</i>
CHAPTER 1 : INTRODUCTION	1
CHAPTER 2 : LITERATURE REVIEW	3
2.1 HSLA (Microalloyed) Steel	3
2.1.1 Introduction	3
2.1.2 Properties Required for HSLA (Microalloyed) Steels	3
2.1.2.a Yield Strength	3
2.1.2.b Low Temperature Toughness	4
2.1.2.c Weldability	5
2.1.3 Production Process for HSLA (Microalloyed) Steels	6
2.1.4 Applications of HSLA (Microalloyed) Steel	12
2.2 Welding of HSLA (Microalloyed) Steels	12
2.2.1 The Weld-Thermal Cycle	12
2.2.2 Effect of Energy Input	14
2.2.3 Structural Changes Due to the Weld Thermal Cycles	16
2.3 Weld Testing	19
2.4 Welding Processes used for Welding of Microalloyed Steels	24
CHAPTER 3 : EXPERIMENTAL PROCEDURES	28
3.1 Material	28
3.2 Equipment	28

3.3	Procedures	30
3.3.1	Sample Preparation	30
3.3.2	Metallography	31
3.3.3	Macro Hardness Measurement	31
3.3.4	Bend Test	31
3.3.5	Macroetching	33
CHAPTER 4 : RESULTS AND DISCUSSION		34
4.1	Weld Deposition Rate	34
4.2	Microstructure	34
4.2.1	Base Metal / Parent Metal	34
4.2.2	Heat Affected Zone (HAZ)	38
4.2.3	Weld Metal	39
4.3	Hardness Profile	40
4.4	Bend Test	41
4.5	Width of Weldment	41
CHAPTER 5 : CONCLUSIONS		60
CHAPTER 6 : SUGGESTIONS FOR FUTURE WORK		61
REFERENCES		62

LIST OF FIGURES

Fig.No.	Title	Page No.
2.1	Typical presentation of TMPC schedule for controlled rolling of HSLA steels	8
2.2	Schematic CCT diagram for control rolled HSLA steels	10
2.3	HAZ regions superimposed on the Fe-C diagram	18
2.4	CCT digram of coarse grained HAZ in C-Mn-Si-Al-Nb steel	20
2.5	Inagaki's experimental tests depicting critical cooling time vs toughness and hardness	25
3.1	Samples cut for microstructural studies, macrohardness testing and bend test	32
4.1	Variation of metal deposited with net heat input	36
4.2	Optical micrograph of base metal	37
4.3	Optical micrographs of HAZ and weldmetal for $H_{net}=2800$ J/mm	42
4.4	Optical micrographs of HAZ and weldmetal for $H_{net}=3000$ J/mm	43
4.5	Optical micrographs of HAZ and weldmetal for $H_{net}=3150$ J/mm	44
4.6	Optical micrographs of HAZ and weldmetal for $H_{net}=3280$ J/mm	45
4.7	Optical micrographs of HAZ and weldmetal for $H_{net}=3450$ J/mm	46
4.8	Variation of macrohardness with distance from weld centre for $H_{net}=2800$ J/mm	52
4.9	Variation of macrohardness with distance from weld centre for $H_{net}=3000$ J/mm	53
4.10	Variation of macrohardness with distance from weld centre for $H_{net}=3150$ J/mm	54
4.11	Variation of macrohardness with distance from weld centre for $H_{net}=3280$ J/mm	55
4.12	Variation of macrohardness with distance from weld centre for $H_{net}=3450$ J/mm	56
4.13	Photograph of samples before and after bend test	57
4.14	Photograph of different zones seen in welded sample after macroetching	58
4.15	Variation of weldment width with net heat input	59

LIST OF TABLES

No.	Title	Page No.
2.1	Expressions for analytical solution of heat flow	15
2.2	Chemical composition of high strength steels and welding electrodes	22
2.3	Tensile properties of submerged arc bead in groove welds deposited in HY80 steel	22
2.4	Tensile properties of submerged arc bead in groove welds deposited in HSLA80 steel	23
2.5	Microhardness of SA bead in groove welds deposited in HY80 and HSLA80 steels	23
3.1	Composition of as received HSLA (microalloyed) steel	28
4.1	Current, welding speed, metal deposited and Hnet for different samples welded at voltage of 30V and with electrode dia 3.15 mm	35
4.2	Macrohardness vs distance from weld centre for load=30kg and Hnet=2800 J/mm	47
4.3	Macrohardness vs distance from weld centre for load=30kg and Hnet=3000 J/mm	48
4.4	Macrohardness vs distance from weld centre for load=30kg and Hnet=3150 J/mm	49
4.5	Macrohardness vs distance from weld centre for load=30kg and Hnet=3280 J/mm	50
4.6	Macrohardness vs distance from weld centre for load=30kg and Hnet=3450 J/mm	51

ABSTRACT

In the present investigation HSLA (microalloyed) steel plate of 6.25 mm thickness has been fusion welded by manual metal arc welding using 3.15 mm diameter low hydrogen basic electrode (AWS E7016) at voltage of 30V and currents of 150, 175, 200, 225 and 250 Amp. The net heat input generated for the above power ratings are 2800, 3000, 3150, 3280 and 3450 J/mm. A constant welding speed approximately 1.87 mm/sec. has been maintained. The welded specimens are subsequently prepared for metallographic examination and hardness testing and bend test.

It is observed that with increase in net heat input the amount of weld metal deposition is increased e.g. for Hnet 2800, 3000, 3150, 3280 and 3450 J/mm the metal deposition rate (Md) is found to be 9.33, 11.23, 11.57, 12.52 and 12.73 respectively.

The microstructure of the base metal has been found to be of typical low carbon steel having ferrite + pearlite. However the grain size of the present steel is relatively finer due to the presence of grain refiner Nb. In all the samples acicular structure and widmanstatten structure has been observed in the HAZ. Typical cast structure has been observed in the weld metal region of all the samples. With increase in net heat input grain coarsening is observed in the weld metal region and in the HAZ region. Coarser dendritic ferrite are clearly visible in higher net heat input samples.

Macrohardness values have been found to decrease from the weld metal region to the base metal. The hardness of the weldmetal is always found to be more than that of the HAZ and hardness of the HAZ is found to be more than that of the base metal. With increase in net heat input the hardness of the weldmetal and HAZ is found to be decreasing.

For Hnet 2800, 3000, 3150, 3280 and 3450 J/mm the peak hardness values in the weldmetal region are found to be 197, 193, 187, 184, 179 VHN. The hardness of the base metal is 164 VHN. The hardness values at a distance of 4 mm from the weld centre line in the HAZ region have been found to be 190, 188, 182, 180 and 177 VHN, for the above mentioned heat inputs respectively. This has been explained on the basis of grain coarsening.

No welded sample has been found to develop any crack during the bend test.

INTRODUCTION

Welding is an operation in which two or more parts are united by means of heat or pressure or both in such a way that there is continuity in the nature of material (metal) between these parts. A filler metal whose melting temperature is of the same order as that of the parent material may or may not be used [1]. The welding processes have been used extensively and popularly for assembling of various structures. Fusion welding is the method of choice for assembling most of the large metal structures such as ships, bridges, nuclear reactors, pipelines, trains and cars etc. In these structures safety and economy are important issues. In simple terms a fusion weld is produced by moving a localized intense heat source along the joint. The chemical composition of weld metal, energy and position of the arc must be carefully controlled to achieve the desired weld quality. Welding offers many advantages over riveting in that air and water tightness, good joining efficiency, economy and without any limit to thickness of the parts to be joined.

However, sometimes welding may create some problems such as cracking and it may lead to reduction of strength in weldment. Extensive research is being conducted for improving welding procedures and to obtain better mechanical properties of the weldment. In the present study, we have focused our attention to the change in microstructure of weldment due to change in heat input in the microalloyed steel. The heat input variation cause complex phase transformations in and around the welded joint producing a wide range of microstructures having different properties. The type of resulting microstructure also depends on many

factors such as weld design, plate thickness, basemetal composition and welding parameters such as current, travelling velocity, preheat temperature etc. thus we can find the variation in microstructure due to change in heat input if other factors are kept constant.

In steels weldability is determined by the microstructural changes that occur in the HAZ. The composition of the base metal in the HAZ remains unchanged, whereas the composition of the weld metal is influenced by the composition of the filler metal and the degree of dissolution attained. In actual welds the microstructure and properties vary considerably from one location to another within the fusion and heat affected zones, depending on thermal history experienced at each point.

High Strength Low Allow (HSLA) (Microalloyed) steels are now becoming important structural materials because of their high strength, toughness at low temperatures and simultaneously maintaining good weldability. Weldability is defined in terms of susceptibility to the various types of cracking during welding fabrication and toughness at heat affected zone (HAZ) [4].

By far the most important technique used in welding construction today is fusion welding. In the present investigation Manual Metal Arc Welding (MMAW) is performed, which is also the most common of the fusion welding processes. Here workpiece is heated to a very high temperature and at a very high rate and the welding operation lasts a very short time followed by rapid cooling under the equivalent to chill cast conditions. As a result of this very severe thermal cycle, the original microstructure and properties of the metal in the region close to the weld arc are changed. The present work is carried out to evaluate the change in microstructure of weldment of microalloyed steel with change in heat input. This is done by subjecting steel samples to various heat inputs during welding. Then hardness test and bend test are carried out. The hardness test shows the resistance to wear of weldment and bend test shows the quality of welded joints.

LITERATURE REVIEW

2.1 HSLA (MICROALLOYED) STEEL

2.1.1 Introduction

HSLA (microalloyed) steels are a group of steels intended for structural application. These steels have specified minimum yield strength of about 275 MPa and sometimes as high as 1035 MPa. These steels contain small amount of alloying elements to achieve high strength in the hot rolled or heat treated conditions [2].

2.1.2 Properties Required for HSLA (Microalloyed) Steels

HSLA (microalloyed) steel plate possesses three fundamental properties. They are

- a) High strength
- b) Toughness at low temperature
- c) Good weldability

Weldability is defined in terms of susceptibility to various types of cracking during welding fabrication and toughness at heat affected zone (HAZ).

These three fundamental properties are discussed below in brief :

2.1.2a Yield Strength

It is the stress corresponding to which material shows plastic deformation. It is related to grain size, degree of strain hardening, distribution of carbide

and nitride particles etc. Mathematically it may be described as follows [3].

$$\sigma_y = \sigma_0 + k_y d^{-1/2} + k'_y d_{SG}^{-n} + k_A f_A \quad \dots(2.1)$$

where d : grains size, d_{SG} : subgrain size, f_A : the volume fraction of the second phase and k'_y , k_y : constants. σ_0 can be express as [2],

$$\sigma_0 = \sigma_{lf} + \Delta\sigma_{ss} + \Delta\sigma_{ppt} + \Delta\sigma_{disl} \quad \dots(2.2)$$

where

- σ_{lf} : lattice friction,
- $\Delta\sigma_{ss}$: solid solution hardening,
- $\Delta\sigma_{ppt}$: precipitation hardening component and
- $\Delta\sigma_{disl}$: dislocation hardening component.

2.1.2.b Low Temperature Toughness

Low temperature toughness is represented by ductile to brittle transition temperature T_{rs} [2]

$$T_{rs} = A' - Bd^{-1/2} - B'd_{SG} + f(z) \quad \dots(2.3)$$

where z is a variable representing volume fraction and morphology to the second phase, and B and B' are constants, A' is given by the following factors :

$$A' = A + \sum a_i x_i + \alpha \Delta\sigma_{ppt} + B\Delta\sigma_{disl} \quad \dots(2.4)$$

where x_i is the content of alloying element, a_i ; α and β are constants and A is a correction factor.

An examination of equation (2.3) reveals as that T_{rs} is governed by the matrix factor, grain and subgrain size factor and factors representing the character of the second phase. It is to be emphasized that all the strength factors decrease toughness, except grain refinement and Ni-addition.

2.1.2.c Weldability

The term weldability describes two different properties. One is low temperature weld cracking which occurs during welding fabrication. This cracking occurs due the combined effects of hydrogen occluded in the HAZ, strain constraint at weld joint and residual tensile stress. However since hydrogen plays a major role in causing low temperature cracking, the crack is very often called hydrogen cracking. The weld-crack susceptibility is given by P_c [3], where

$$P_c = P_{cm} + t/600 + [H] \quad \dots(2.5)$$

where, t is the plate thickness in mm representing the degree of strain constraint and $[H]$ is diffusible hydrogen in weld metal of 100 g. P_{cm} is called weld-crack, chemical composition index [3], and is given by

$$P_{cm} = C + \frac{Si}{30} + \frac{Mn}{20} + \frac{Cu}{20} + \frac{Ni}{60} + \frac{Co}{20} + \frac{Mo}{15} + \frac{V}{15} \quad \dots(2.6)$$

P_c represents weld susceptibility (for the low alloy steels) to weld cracking (cold).

Carbon equivalent (C_{eq}) is also often used to describe the susceptibility to weld cracking. However, C_{eq} is more suitable to describe the maximum hardness at HAZ, and accordingly ductility rather than crack susceptibility. C_{eq} is given by [3].

$$C_{eq} = C + \frac{Mn}{6} + \frac{Cr + Mo + V}{5} + \frac{Ni + Cu}{15} \text{ (in wt. \%)} \quad \dots(2.7)$$

Z. Zaczek and J. Cwiek made a detailed study on HAZ hardness in welds of quenched and tempered HSLA steels. The results of investigation on HSLA Q & T steels 12-25 mm. in thickness and with yield pt. ranging from 420 to 690 MPa shows that the carbon equivalent formula given by k Lorentz and C. Duren

$$CE = C + \frac{Mn}{16} + \frac{Si}{23} + \frac{Ni}{34} + \frac{Cr}{11} + \frac{Cu}{19} + \frac{Mo}{12} + \frac{V}{6} \quad \dots(2.8)$$

is the most reliable for these steels in predicting cold cracking in HAZ and maximum HAZ hardness increases with growth of the carbon equivalent [5].

The other property of weldability is the toughness in HAZ, which governs the performance of weld-joint and thereby welded structure. Toughness at HAZ is markedly deteriorated due to coarse grain structure and the formation of brittle, hard martensite. In general strengthening of base metal through the additions of alloying contents definitely decreases toughness.

2.1.3 Production Process for HSLA (Microalloyed) Steels

In order to meet the fundamental properties of HSLA steels such as higher strength, improved toughness, ductility, formability and increased weldability, the carbon content is kept low (0.03-0.15) pct.; moreover one or more of the strong carbide forming elements which are stable at high temperature such as vanadium, titanium and niobium along with a group of solid solution strengthening elements such as manganese and silicon are added to steel [2].

In order to meet the contradictory requirements of these steels, desired strength is achieved through refinement of ferrite grain size, produced by additions of microalloying elements and in combination with various forms of thermo mechanical processing. This procedure has made it possible to improve the resistance of steels to hydrogen assisted cold cracking, stress corrosion cracking (SCC), the brittle fracture initiation in the weld heat affected zone without

lowering the base metal strength, ductility or low temperature toughness [2].

The bulk of structural steels may be produced by one of the following routes [4].

1. Hot rolling, without subsequent heat treatment,
2. Controlled rolling, i.e., rolled at a temperature in a narrow range so that a fine grain size is produced.
3. Direct normalising of hot rolled product e.g. forced air cooling.
4. Normalising of hot rolled product after cooling to ambient temperature.
5. Quenching and tempering
6. Control quenching, to produce a bainitic structure.

The most important process is the control rolled process where a careful control of time-temperature-deformation sequence is carried out. The main purpose of controlled rolling is to refine grain structure and thereby increase both the strength and toughness of steel in the hot rolled condition to a level equivalent to, or better than those of highly alloyed and quenched and tempered steels [4].

The presence of microalloying elements in low carbon steel would produce an extremely fine dispersion of small and stable microalloy carbides, nitrides and/or carbonitride precipitates which effectively influence the grain coarsening and cause pinning of austenite boundaries during controlled rolling. Such steels subsequently transform into a fine grained ferrite structure. The controlled rolling practice for steels of suitable composition is shown schematically in Fig.2.1 [6].

Presence of manganese suppresses austenite to ferrite transformation temperature and retards the rate of transformation thereby leading to refinement of the ferrite grain size [6]. Addition of (1.5-2.0) percent of manganese may produce acicular or bainitic structures. In case of niobium and vanadium, carbonitrides of these elements may precipitate in austenite during transformation, or in the ferrite after transformation is complete [4].

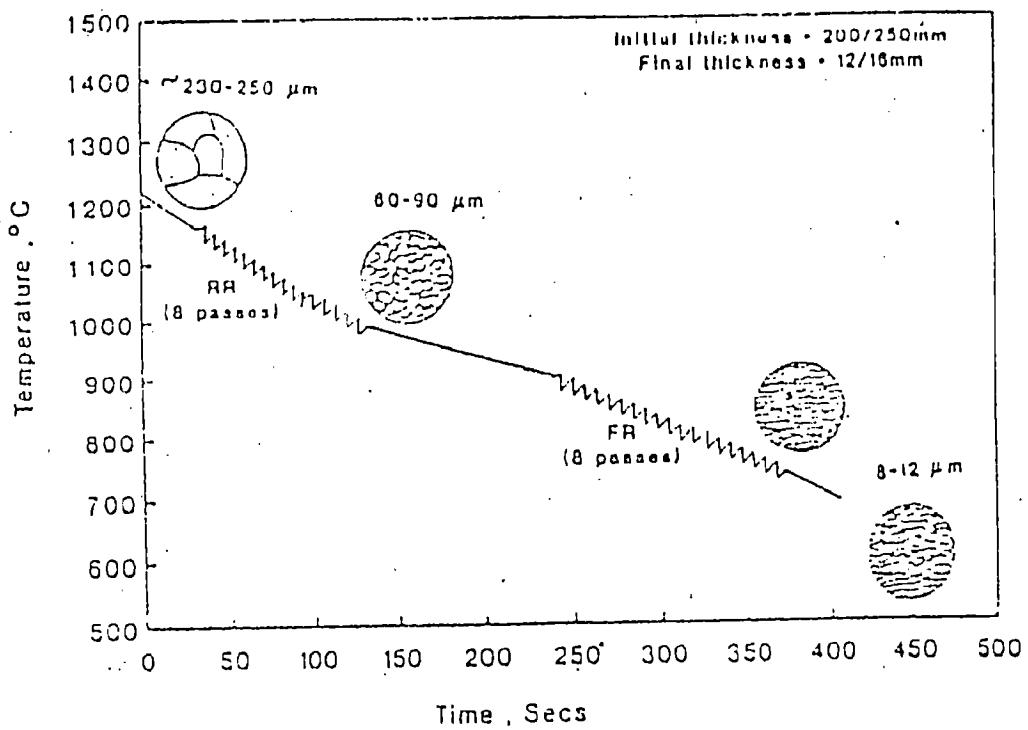


FIGURE 2.1 Typical presentation of TMPC schedule for controlled rolling of HSLA steels

The transformation behaviour of a controlled rolled microalloyed steel may be represented by critical cooling transformation (CCT) diagram as shown in Fig.2.2. The transformed microstructure may include pearlite, polygonal ferrite, acicular ferrite, bainite and martensite depending on the processing route and steel chemistry.

The major strengthening mechanism in controlled rolled HSLA steels includes the following [4].

1. Grain refinement
2. Precipitate hardening by strain enhanced precipitation of microalloy carbonitrides in ferrite.
3. Solid solution strengthening from Mn, Si and uncombined nitrogen.
4. Dislocation substructure strengthening
5. Strain aging

The contribution to strength has been suggested [4] for a Nb microalloyed and controlled rolled HSLA steel by the given equation

$$\begin{aligned} \sigma_y (550 \text{ MPa}) = & \sigma_L (6\%) + \sigma_{\text{solid soln}} (25\%) + \sigma_{\text{ppt. hard}} (6\%) + \sigma_{\text{text}} (8\%) \\ & + \sigma_{\text{dislocation}} (8\%) + kd^{-1/2} (47\%) \quad \dots(2.9) \end{aligned}$$

The grain size achieved through controlled rolled process is around 5-9 μm [6].

Grain Refinement in HSLA Steels

Grain refinement is accomplished by the addition of Nb, V and Ti. Addition of Nb is favoured because the solubility of Niobium Carbonitrides (Nb(CN)), is less than the carbides or nitrides of V and Ti [7]. In HSLA steels containing Nb, the alloying elements Nb, C and N remain in solution in austenite during hot rolling at higher temperatures. However during the course of hot rolling, carbide, nitride

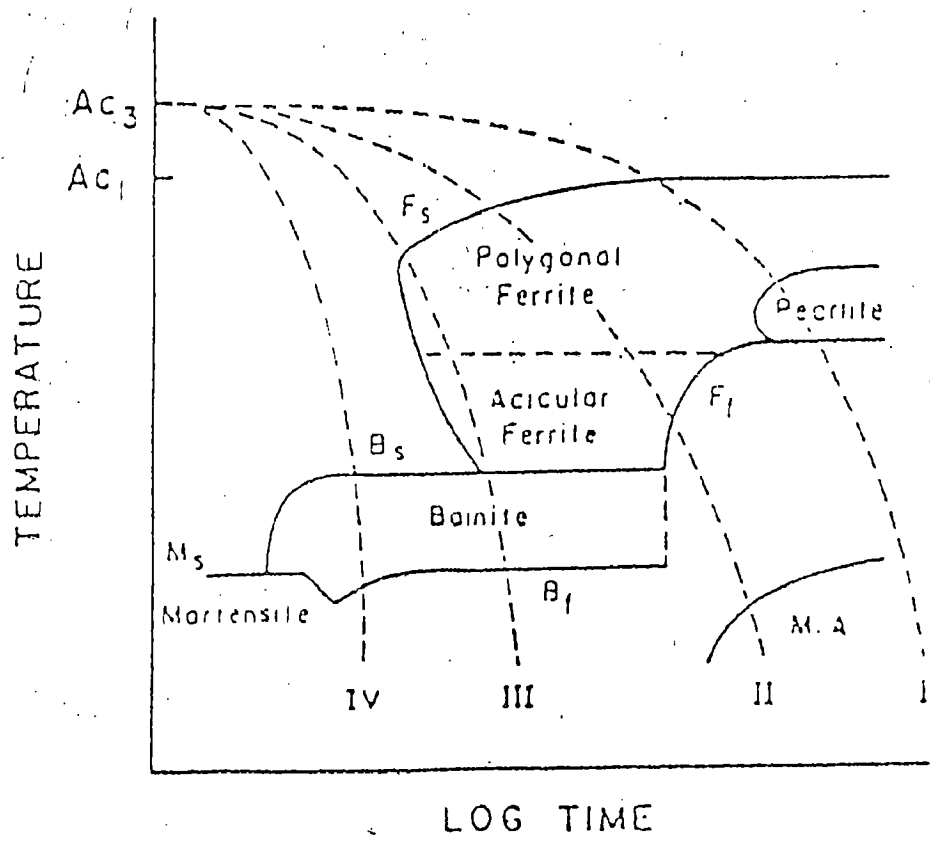


FIGURE 2.2 Schematic CCT diagram for control rolled HSLA steels

or carbonitride of Nb may precipitate in the deformed austenite matrix. The precipitate particles hinder the growth of austenite grains. Due to presence of particles, the recrystallization process in the lower austenite region is suppressed. The γ - α transformation occurs in unrecrystallised austenite. A higher driving force is therefore affected for the austenite to ferrite transformation. The solubility of microalloying elements in austenite is in the increasing order of Nb, Ti, V. The resulting ferrite grain size of HSLA steel microalloyed with Nb is the least [7].

Precipitation Strengthening in HSLA Steels

Ultra fine grain size imparts greater strength and toughness to the HSLA steels. The carbide, nitride or carbonitride particles of microalloying elements, although are effective in controlling grain growth, they do not cause strengthening because they are too large and widely spaced [7]. The particles that contribute to strengthening are those that form during austenite to ferrite transformation at lower temperatures when the steel passes through the (γ + α) phase field during cooling. Because of its higher solubility vanadium carbide precipitates only during the γ - α transformation.

In addition to the above strengthening mechanisms, controlled deformation and heat treatment processes can be utilized to impart greater strength and toughness to HSLA steels. One of these processes is controlled rolling and controlled cooling. The purpose of controlled hot rolling of ferritic-pearlitic steel is to develop fine uniform ferrite grains coupled with precipitation hardening. The situation demands heavy deformation and low finishing temperature in the austenite region below about 950⁰C. Heavy deformation leads to fine grain size of the recrystallised austenite and lower finishing temperature ensures that Nb(CN) precipitate particles do not become usually large and grain growth of recrystallised austenite is restricted [7].

2.1.4 Applications of HSLA (Microalloyed) Steel

1. Controlled rolled plates of C/Mn/Nb steel are used extensively for production of large diameter linepipe.
2. Heavy structural and pressure vessel plates are produced.
3. Offshore structures as submersible drilling rigs, stationary production platform, storage tanks, crane, ships etc.
4. Electric power transmission towers.
5. Truck bodies, truck-spring cover plate, Truck-spring seat, Bumper.
6. Heat exchangers
7. Gas cylinders
8. Industrial bins, containers
9. Ship hull structural material.

2.2 WELDING OF HSLA (MICROALLOYED) STEELS

2.2.1 The Weld-Thermal Cycle

Arc welding is a process in which a very intense moving heat source is applied to the work piece. By studying heat flow during welding, useful results can be obtained. Many investigators have made detailed study of heat flow in welding. The solutions obtained are useful in predicting thermal cycles and base metal and hence in predicting microstructure of heat affected base metal and other related problems associated with welding.

The basic equation to describe heat flow in a solid body i.e. Laplace equation is given as follows :

$$\frac{\partial T}{\partial t} = \frac{1}{\rho c_p} \left[\frac{\partial}{\partial x} \left(k \frac{\partial T}{\partial x} \right) + \frac{\partial}{\partial y} \left(k \frac{\partial T}{\partial y} \right) + \frac{\partial}{\partial z} \left(k \frac{\partial T}{\partial z} \right) \right] + Q_g \quad \dots(2.10)$$

where,

T = Temperature (k)

t = Time (sec.)

k = Thermal conductivity (w/m-k)

c_p = Specific heat (J/kg-k)

ρ = Density (kg/m³)

x,y,z = Co-ordinates in three perpendicular direction (m)

Q_g = Rate of heat generation per unit volume of the body (J/s-m³)

Rosenthal [8] was the first to report an analytical solution by making the following assumptions :

1. The heat source moves with a constant speed along a line on the surface of a large body.
2. Thermal properties of the material remain constant.
3. No heat is lost by radiation and convection to surroundings.
4. Quasi steady state is reached, i.e., temperature distribution with reference to heat source does not change with time.

Rosenthal modified the differential equation for a quasi stationary state w.r.t. moving coordinates and obtained the following :

$$-v \frac{\partial T}{\partial W} = \alpha \left[\frac{\partial^2 T}{\partial W^2} + \frac{\partial^2 T}{\partial y^2} + \frac{\partial^2 T}{\partial z^2} \right] \quad \dots(2.11)$$

where,

$$w = x - vt$$

$$\alpha = [k/\rho c_p]$$

= Thermal diffusivity of the solid (m²/s)

$$\rho = \text{Density of solid (kg/m}^3\text{)}$$

w = Distance from heat source in x-direction (m)

v = Velocity of heat source

t = time (sec.)

Rosenthal solved equation (2.11) under a few simple cases and these are tabulated in Table 2.1.

2.2.2 Effect of Energy Input

The dominant factor governing all significant thermal events in welding is the energy input which affects peak temperature distribution, cooling rate and solidification time. Metallurgical considerations generally favour low arc energy input; the extent of HAZ is minimized and weld metal properties are enhanced through production of fine dendrite structure. Simple economics favour the use of large passes (high energy input) because they are associated with high deposition and production rates. Also there can be metallurgical benefit from reduced cooling rates at high H_{net} values.

The higher the heat input rate, lower is the cooling rates and longer the weld pool. Increased cooling rates increases the risk of hydrogen induced cracking. High heat input rates give less HAZ cracking in welding of alloy steels. If the cooling rate can be measured then by superimposing this on the CCT diagram of the steel of interest it would be possible to predict the final microstructures. The grain size in weld metal as well as HAZ is directly affected by heat input rate. A higher heat input rate gives a longer thermal cycle and tend to generate a coarser structure. So in steel welding an optimum has to be struck between grain size and cooling rate [4,9].

The extent to which high tensile steels are weakened during fusion welding is governed by the width of region in the HAZ which is heated to the temperature at which high temperature tempering develops most in the metal (500-770°C).

Reducing the unit energy input during welding, with the thickness of the steel unchanged, narrows the HAZ and the strength of the joint increase. We know that, when butt welds in thin metal are made by a single pass process, the unit energy input can be adjusted over a wide range while still achieving full penetration of the weld edges.

Plate Thickness	Type of heat flow	Expression for analytical solution of heat flow
Thick	3-dimensional	$T - T_0 = \frac{Q}{2\pi k} e^{-(v/2\alpha)w} \frac{e^{-(v/2\alpha)R}}{R}$ *
Finite thickness	2.5 dimensional	$T - T_0 = \frac{Q}{2\pi k} e^{-(\frac{V}{2\alpha})w} \left[\frac{e^{-(\frac{V}{2\alpha})R}}{R} + \sum_{n=1}^{\infty} \frac{e^{-(\frac{V}{2\alpha})R_n}}{R_n} + \frac{e^{-(\frac{V}{2\alpha})R_n'}}{R_n'} \right]$ **
Thin	2-dimensional	$T - T_0 = \frac{Q/s}{2\pi k} e^{-(\frac{V}{2\alpha})w} k_0\left(\frac{V}{2\alpha} r\right)$ ***

$$R = \sqrt{w^2 + y^2 + z^2}$$

Q = Strength of the heat source (J/s)

*

$$R_n = \sqrt{w^2 + y^2 + (2nt - z)^2}$$

$$R_n' = \sqrt{w^2 + y^2 + (2nt + z)^2}$$

t - plate thickness

**

$$r = \sqrt{w^2 + y^2}$$

K_0 = is modified Bessel function of the second kind and zero order.

S = plate thickness.

Table 2.1: Expression for analytical solution of heat flow.

Hunt et al. [10] examined the sensitivity of the weld metal microstructure and mechanical properties to variations in both heat input and weld dilution in submerged arc welding of microalloyed steel (ASTM A710 Grade A) by commercial solid welding wires of oerlikon Tibor 22 and flux oerlikon OP121TT. They found that the weld metal hardenability is not significantly affected by an increase in weld meal dilution from 40% to 70%. Low dilution welds (double pass) exhibited a slightly larger mean inclusion size than to high dilution (single pass) welds. The low dilution welds also exhibited higher fractions of finer acicular ferrite compared to high dilution welds. The microstructure and toughness of low dilution welds were found to be independent of heat input while high dilution welds were found to be very sensitive to variations in heat input. The result of this study point out the complexity of phase transformation in microalloyed steel weld metal subjected to multiple thermal cycles [10].

2.2.3 Structural Changes Due to the Weld Thermal Cycles

Metallurgically, there are three distinct zones in a welded part, namely :

1. Weld metal
2. Heat affected zone
3. Unaffected basemetal

Weld Metal

The weld metal is that part of weldment that has melted and resolidified during the welding operation. The microstructure and properties of weld metal depends on complex interaction between several important variables such as the total alloy content, the concentration of different solute elements, prior austenite grain size and weld thermal cycle [11].

Heat Affected Zone

The heat affected zone (HAZ) is that part of the base metal adjacent to the

weld metal which has been heated during welding to a high temperature. It has undergone significant and detectable structural change, but has generally not become molten. The properties of the region are determined by the austenite grain size, matrix composition and cooling rate. The precipitation will be effective in restricting grain growth unless it coarsens or dissolves into the matrix. Depending on steel composition, Nb (CN) can restrict grain growth up to a temperature of 1200-1250°C whereas V (CN) is effective only up to 900°C [4].

The time span to cool from 800°C to 500°C in the weldment (t_{8-5}) has now been widely adopted in welding research [12]. Most of the transformations in plain carbon steels occur in the temperature interval of 800-500°C and time of cooling in this temperature range is critical.

Depending on the peak temperature that has been reached, the heat affected zone can be divided into four distinct zones [13].

These are :

1. Coarse-Grained HAZ (CGHAZ), adjacent to the fusion line.
2. Fine-Grained HAZ (FGHAZ), above AC_3 and below grain coarsening temperature.
3. Inter-critical HAZ (ICHAZ), between AC_1 and AC_3 temperature range.
4. Sub critical HAZ (SCHAZ), below AC_1 temperature different subzones of HAZ are shown in Fig.2.3

Coarse Grained HAZ

This zone experiences peak temperatures between 1100°C and 1450°C. Temperature of this range produces a coarse grained austenite which because of low density of grain boundaries, tends to preclude extensive transformation to ferrite during cooling. Further peak temperature of this order causes dissolution of all the precipitates thus increasing the hardenability of steel [13]. Phases that are observed in this region include equiaxed or polygonal ferrite, Widmanstätten ferrite, bainitic ferrite and lath martensite. In addition the carbon enriched

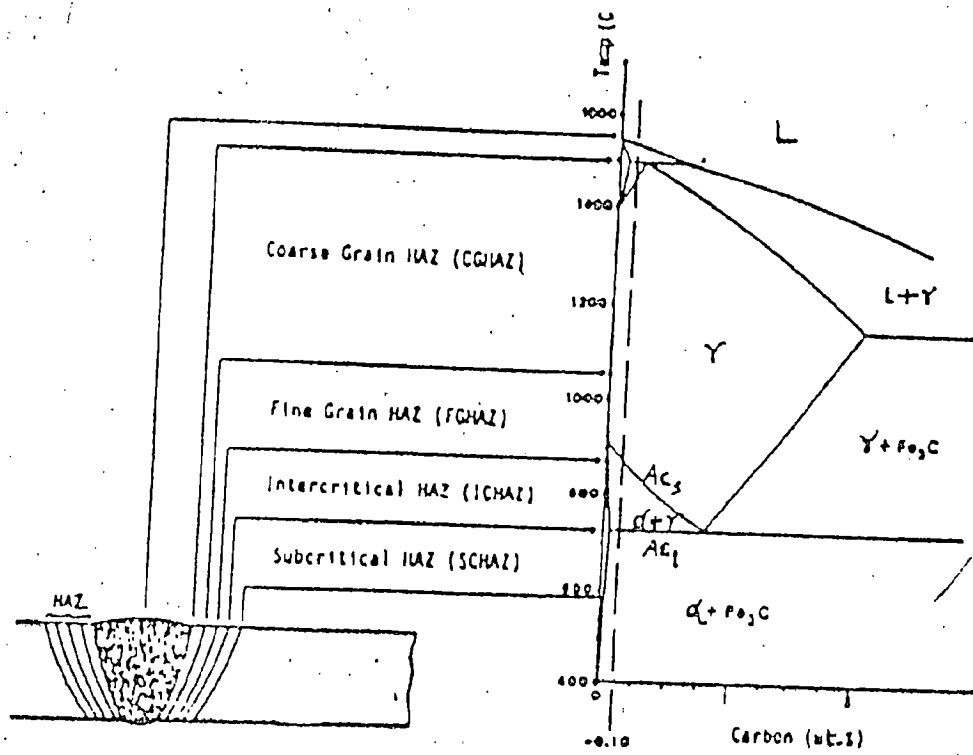


FIGURE 2.3 HAZ regions superimposed on the Iron-Carbon diagram

phases or minor phases associated with the above mentioned ferrites may transform to pearlite, degenerated pearlite, carbides or martensite-austenite (M-A). Fig.2.4 shows CCT diagram applicable to CGHAZ region in a C-Mn-Si-Al-Nb steel [14]. Brownrigg and Boelen [15] observed that at a cooling rate corresponding to shielded arc welding (SAW) at 3.5 KJmm^{-1} on a plate of 50 mm thickness, the microstructure is bainite.

Fine-Grained HAZ

This zone corresponds to a peak temperature in the temperature range of 850°C - 950°C . At these temperatures Nb(CN) restricts the grain growth of austenite. The austenite grain size is small and equiaxed which leads to the formation of polygonal ferrite.

Inter Critical HAZ

This zone corresponds to a peak temperature between AC_1 and AC_3 . Only the carbon rich constituents form austenite.

Sub Critical HAZ

This zone corresponds to a peak temperature below AC_1 . Growth of precipitate particles, dislocation annihilation and strain aging are the only processes that are effective in this temperature range.

2.3 WELD TESTING

Welded joints in a welded structure are expected to possess certain service related capabilities. Welded joints are generally required to carry loading of various types in the weld is subject to stress of either a simple or complex character. Moreover, a finished weld is not always as good or as bad as it may appear to be on its surface. It is therefore necessary to find out how satisfactory or sound the weld is. For this purpose certain weld testing

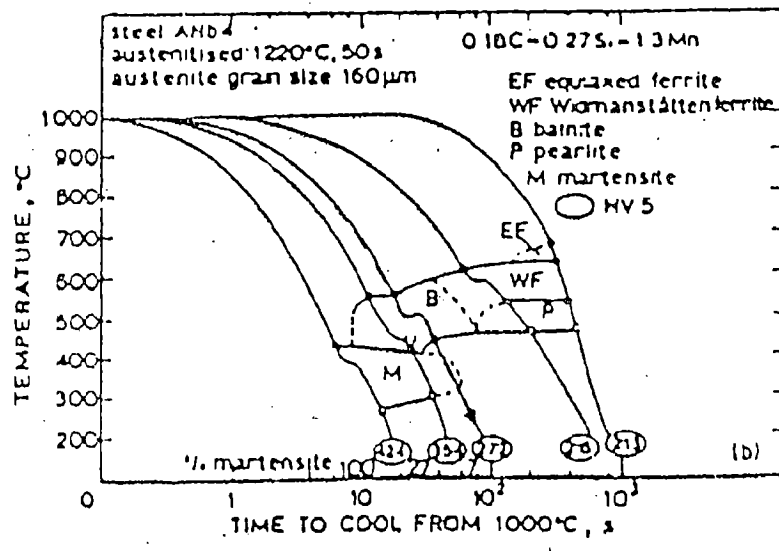


Figure 2.4 CCT diagram for coarse grained HAZ in C-Mn-Si-Al-Nb steel[14]

procedures have been discovered and standardized to estimate the expected performance of welded structure.

The bend test is an easy and inexpensive test to apply. It shows the quality of the welded joints. It shows ductility of welded zone, weld penetration, fusion, crystalline structure (of fractured surface) and strength etc. on the other hand hardness test gives an idea of resistance to wear of weldment. Hardness values can give information about the metallurgical changes caused by welding [16].

Many researchers have adopted different techniques to assess the different zones of weldment. Gianetto et al. [17] made a detailed assessment of the influence of composition and energy input on the structure and properties of single pass submerged arc bead in groove welds produced on HY80 and HSLA80 steels. Dilution from the base plate produced a marked variation in weld metal composition between the HY80 and HSLA80 series of welds, which resulted in major differences in microstructure and mechanical properties. The low temperature notched toughness was poor for 1 and 4 KJ/mm welds with an improvement observed at intermediate energy input. The poor notch toughness was attributed to the formation of hard lath martensite with high yield strength. Intermediate energy input welds consisted of fine bainite microstructure with lower yield strength, which provided improved notch toughness. The HSLA80 welds showed a small decrease in yield strength with increasing energy input and superior notch toughness independent of energy input. This occurred as a result of transformation to a high proportion (80%) of acicular ferrite with limited continuous/discontinuous grain boundary ferrite. The microhardness data for HY80 weld metals showed a pronounced decrease between 1 and 2 KJ/mm welds and supported the observations of a change in microstructure from mainly lath martensite to predominantly bainite. Only a slight decrease in micro hardness was observed for HSLA80 welds deposited at 1 to 4 KJ/mm due to the coarser structure in latter weld. All these results are tabulated in Tables 2.2, 2.3, 2.4 and 2.5.

Table 22— Chemical Compositions of High-Strength Steels and Welding Electrode

Material	Element wt-%									
	C	Mn	Si	S	P	Ni	Cr	Mo	Cu	N
Y80	0.17	0.30	0.19	0.014	0.007	2.59	1.53	0.42	0.03	0.1
SLA80	0.06	0.50	0.27	0.004	0.007	0.92	0.66	0.25	1.02	0.1
IOS-1	0.07	1.57	0.52	0.004	0.004	1.86	0.03	0.28	0.06	
Y80 ^(a)	0.12-	0.10-	0.15-	0.002-	0.020	2.00-	1.00-	0.20-	0.25	
IL-S-16216J	0.18	0.40	0.35	0.020		3.25	1.80	0.60		
SLA80 ^(a)	0.05	0.40-	0.40	0.006	0.020	0.70-	0.60-	0.15-	1.00-	0.1
IL-S-24645A		0.70				1.00	0.90	0.25	1.30	0.1
IOS-1 ^(a)	0.08	1.25-	0.20-	0.01	0.01	1.40-	0.30	0.25-	0.30	
IL-E-23765/2C		1.80	0.55			2.10		0.55		

Table 23— Tensile Properties of Submerged Arc Bead-in-Groove Welds Deposited in HY80 Steel

Weld No.	Energy Input (kJ/mm)	Yield Strength (MPa)	Ultimate Strength (MPa)	Elongation (%)	Reduction in Area (%)
HY80-1	1	875	1124	18	54
HY80-2	2	745	930	24	59
HY80-3	3	680	858	25	64
HY80-4	4	666	867	25	63

Table 2.4 Tensile Properties of Submerged Arc Bead-in-Groove Welds Deposited in HSLA80 Steel

Weld No.	Energy Input (kJ/mm)	Yield Strength (MPa)	Ultimate Strength (MPa)	Elongation (%)	Reduction in Area (%)
HSLA80-1	1	640	806	25	64
HSLA80-2	2	618	756	28	66
HSLA80-3	3	607	720	27	65
HSLA80-4	4	595	710	28	65

Table 2.5 Microhardness of Submerged Arc Bead-in-Groove Welds Deposited in HY 80 and HSLA80 Steels

Energy Input (kJ/mm)	Microhardness, DPH	
	HY80	HSLA80
1	369 (360-380)	265 (258-271)
2	309 (301-315)	248 (244-251)
3	289 (284-296)	239 (236-242)
4	283 (280-292)	236 (231-240)

Inagaki et al. [18] did a large amount of experimental work determining a relationship between energy absorbed during a weld joint bend test and the cooling time of the weld joint-fusion line. In their study total bend angle and Charpy impact tests were done on samples to verify that cooling time longer than t'_{8-5} created larger bend angles and more absorbed energy - Fig.2.5. Also from these curves it can be observed that hardness decreases with cooling times greater than t'_{8-5} . Therefore he suggested to keep toughness at a maximum use t'_{8-5} as minimum, but to keep strength of steel up (related to hardness) attempt to keep t'_{8-5} as the maximum. It then can be concluded that t'_{8-5} is a cooling time to optimize weld joint strength for different kind of loading and steels.

2.4 WELDING PROCESSES USED FOR WELDING OF MICROALLOYED STEELS

The factors which are generally considered for selection of a welding process are hydrogen induced cracking, interruption of heating cycle, lamellar tearing etc.

On basis of these consideration these steels can be welded by all commonly known arc welding processes. Manual metal arc, gas metal arc, submerged arc. Electro gas and electroslag welding can be used with certain loading restrictions for bridge and other applications. These steels can also be joined by resistance spot, seam, projection, upset and flash welding [19].

Many of the existing procedure require use of high welding heat input (submerged arc, electro gas, electroslag) which in presence of microalloyed steels generally give toughness problems in welds. More suitable processes in this respect have been developed (electron beam, laser) but their application is limited due to their high cost, necessity of skilled technician and some operational difficulties [20].

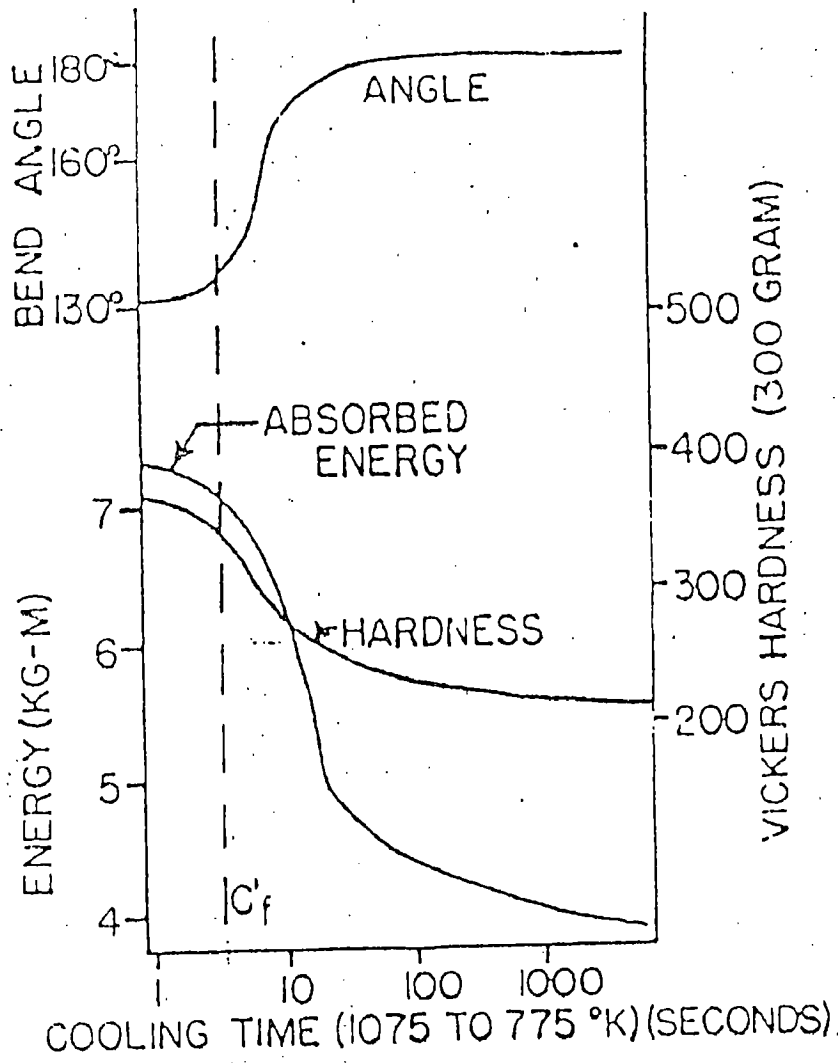


Figure 2.5 Inagaki's experimental tests depicting critical cooling time vs. toughness and hardness[18]

Submerged Arc Welding

The SAW is used mostly for the welding of microalloyed steel. It has got wide application such as in shipbuilding industry, vessels and tanks for pressure and storage use. Metal thickness from 1.6 mm to 12 mm can be welded with no edge preparation with this method. With edge preparation welds can be made with a single pass on material from 6.4 mm through 25 mm. When multipass technique is used the maximum thickness is practically unlimited [21].

In welding of microalloyed steel by SAW, flux exerts a great influence on the toughness of weld metal and it has been shown by studies that Ti has a beneficial effect [22].

For best HAZ and weld metal toughness, microstructure is the main parameter. The minimum welding energy (i.e. the shortest cooling time) compatible with cold cracking and the integrity of the joint is desirable. For weld metal, microstructural refinement will also be achieved through proper welding wire alloying. Mo being the most promising element for this purpose [23].

Electroslag Welding

Electroslag process is also used for welding of these steels. This process has lot of advantages as high metal deposition rate, ability to weld thick material in one pass, high quality weld, mechanised process etc. The thickness range of metal is 20 mm to 950 mm [21].

Spot Welding

In automobiles the weight reduction is needed but safety requirement generally result to wt. increase. Microalloyed steel can give high strength, good ductility and toughness. Due to the above said requirement spot welding is used and this steel shows good weldability but the fatigue strength of weldment is not good.

Manual Metal Arc Welding

MMAW is also used in fabrication of this steel. Low hydrogen electrodes are used and no problems which can be attributed to arc transfer has been reported. Lamellar tearing problem is also not found. The problem encountered is that of meeting the low HAZ hardness requirement.

2.5 FORMULATION OF THE PROBLEM

After reviewing the available literature it was observed that very little work has been done on welding of H.S.L.A. (microalloyed) steels. Most of the work is concentrated on the grades of H.S.L.A. steels which are alloyed with somewhat higher percentage of alloying elements (other than microalloying elements). Also very little work has been done on effect of heat input on microstructure of weldment of H.S.L.A. (microalloyed) steels welded by Manual Metal Arc Welding process. Most of the work is done on Submerged Arc Welding process.

Being a very important structural material, H.S.L.A. (microalloyed) steels are welded frequently and welds of these steels are found to be very sensitive to variations in heat input. Thus this study has been carried out to find the effect of heat input on microstructure of weldment in welding of H.S.L.A. (microalloyed) steels.

EXPERIMENTAL PROCEDURES

Details of experiments designed to find the effect of heat input on the microstructure of weldment in welding of HSLA (microalloyed) steels are presented in this chapter. This includes microstructural study macrohardness testing and bend test.

3.1 MATERIAL

The composition of HSLA (micro alloyed) steel used in the study is shown in Table 3.1. This steel was obtained from Bokaro Steel Plant.

Table 3.1 Composition of HSLA (microalloyed) steel

Plate Thickness (mm)	C	Si	Mn	P	S	Nb	Fe
6.25	0.1	0.12	0.9	0.03	0.03	0.02	Rest

3.2 EQUIPMENT

The following equipments were used in the experimental work :

Power Source

A welding set of type GES-350A of the following specifications was used :

Motor

Output c.r. 100% 14 KW

Speed 1450 r.p.m.

Power Factor 0.87

Frequency 50 cps

Voltage 440 V

Current 275 A

Welding Generator

Welding current

i.e. 55% 350 A

c.r. 100% 260 A

Voltage 30V

Welding current range

80 - 400 A

Weight 260 Kg

Welding Electrode : Medium-heavy coated, all position hydrogen controlled electrode of following specification was used :

AWS	E7016
IS	EB5426H ₃ X
Dia	3.15 mm
Length	450 mm

Power Saw : All cutting operation were carried out on power saw with HSS, 300×25×1.25 blade of 10 TPI.

Electric Oven : Of temperature range 50-300⁰C was used to remove moisture in the welding electrodes.

Disc Polisher : Cloth polishing carried out on sylvet cloth wrapped over rotating wheel of disc polisher.

MeF₃ Reichert : Optical microscope attached with camera was used for optical microscopy.

Vickers Hardness Testing Machine : was used to find vicker hardness no.

3.3 PROCEDURES

3.3.1 Sample Preparation

The plate was cut into 10 pieces of dimension 6cm×2.5cm×0.6 cm. The edges of two pieces for each set were cut to form a v-groove having 60° included angle with the help of a shaper m/c.

Initial weight of each set of plates were taken with the help of a physical balance.

Welding Procedure

The electrodes were kept in an electric oven at a temperature of 125-150°C for 4 hrs to remove moisture.

The welding was of single pass, single vee butt joint using above said electrode.

The samples were welded at five different currents and avoiding large change in welding speed to get five different heat input.

Welding speeds were calculated by recording the time required for welding each set with the help of an electronic stop watch which had an accuracy of 1/100th of a second.

While welding, the electrodes were kept at an angle of approximately 20 degrees with the vertical.

The final weight of each sample was taken and thus the amount of metal deposited per unit length was calculated. Also heat input-rates were calculated using equation (3.1)

$$H_{net} = \frac{EI}{V} \text{ J/mm} \quad \dots(3.1)$$

where

E = Voltage (V)

I = Current (Amp.)

V = Welding speed (mm/sec.)

Total 10 samples were cut, 2 from each set at a distance of 1.5 mm and 3.0 mm, of 1.5 mm width in the transverse direction, from one end (Fig.3.1).

3.3.2 Metallography

The samples were first levelled using a surface grinder and then properly ground on abrasive belt. Then these samples were imparted surface finish of required standard using amery papers upto 4/0 number and in definite sequence followed by cloth polishing carried out on sylvet cloth using 0.1 μm size alumina powder suspension. After etching with 2% Nital, washing and drying, the samples were ready for metallographical studies. MeF₃ Reichert optical microscope was used for taking photographs and observation revealed typical microstructural features.

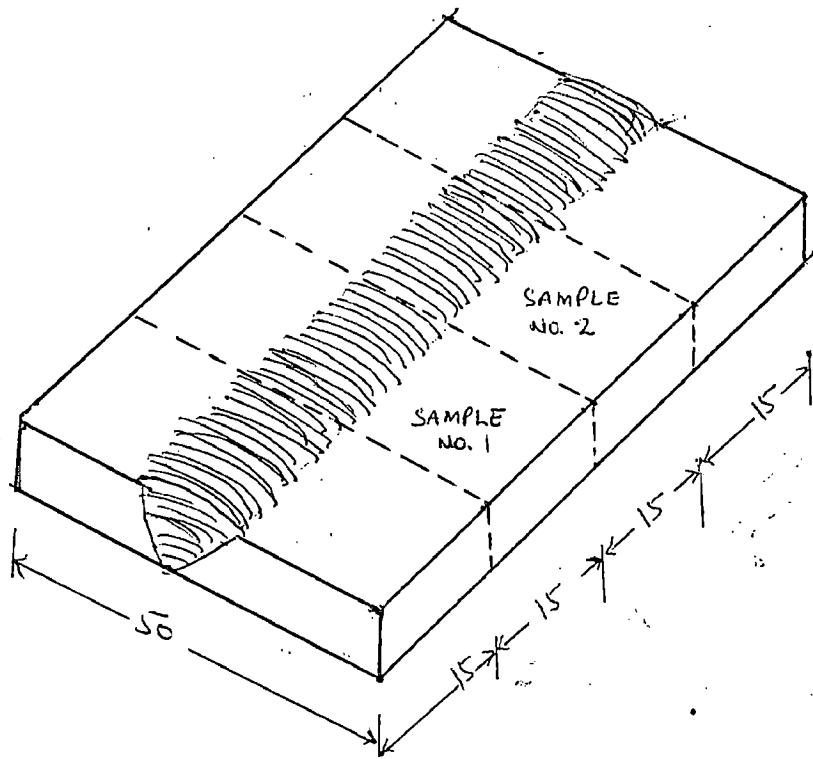
3.3.3 Macro Hardness Measurement

Macro hardness measurements across weldmetal, HAZ and parent metal were taken. For each sample vicker hardness No. (VHN) from one end to other were taken on vicker hardness testing machine using 30 kg load and variation with distance is plotted.

3.3.4 Bend Test

Free bend test was conducted on a tensile testing machine by exerting a load of 6 tonne on each sample and soundness of weld metal, the weld junction and heat affected zone was assessed. Photograph showing the samples before and after bend test was taken.

FIG. 3.1 Samples cut for microstructural studies, macrohardness testing and bend test



3.3.5 Macroetching

A samples was macroetched with 2% Nital solution exposing it for 15 min. Photograph of macroetched sample was taken in which the different zones are clearly visible.

RESULTS AND DISCUSSION

4.1 WELD DEPOSITION RATE

In the present work it is observed that the weld deposition increases as the net heat input increases. A straight line relationship has been observed by regression analysis of the data.

The relationship between heat input and metal deposited may be expressed by a simple mathematical expression :

$$Md = 5.166 \times 10^{-3} H_{net} - 4.725$$

Here Md = Metal deposited (gm)

Hnet = Net heat input (J/mm)

The variation of metal deposited with net heat input is shown in Fig.4.1 and data is given in Table 4.1. This relation is valid in Hnet range from 2800 J/mm to 3450 J/mm.

4.2 MICROSTRUCTURE

4.2.1 Base Metal / Parent Metal

The microstructure of the base metal of the microalloyed steel in the as received condition consists of ferrite and pearlite as shown in Fig.4.2. Here the white areas show ferrite and black areas represent pearlite. The volume fraction of pearlite in this steel is estimated to be 15%. This volume fraction measurement

Sample No.	Current (Amp)	Welding Speed (mm/Sec.)	Metal Deposited (gm.)	Hnet (J/mm)
1	150	1.607	9.33	2800
2	175	1.750	11.23	3000
3	200	1.904	11.57	3150
4	225	2.057	12.52	3280
5	250	2.173	12.73	3450

Table 4.1 Current , Welding speed , Metal deposited and Hnet (Calculated) for different samples welded at constant voltage of 30V and with electrode dia 3.15 mm.

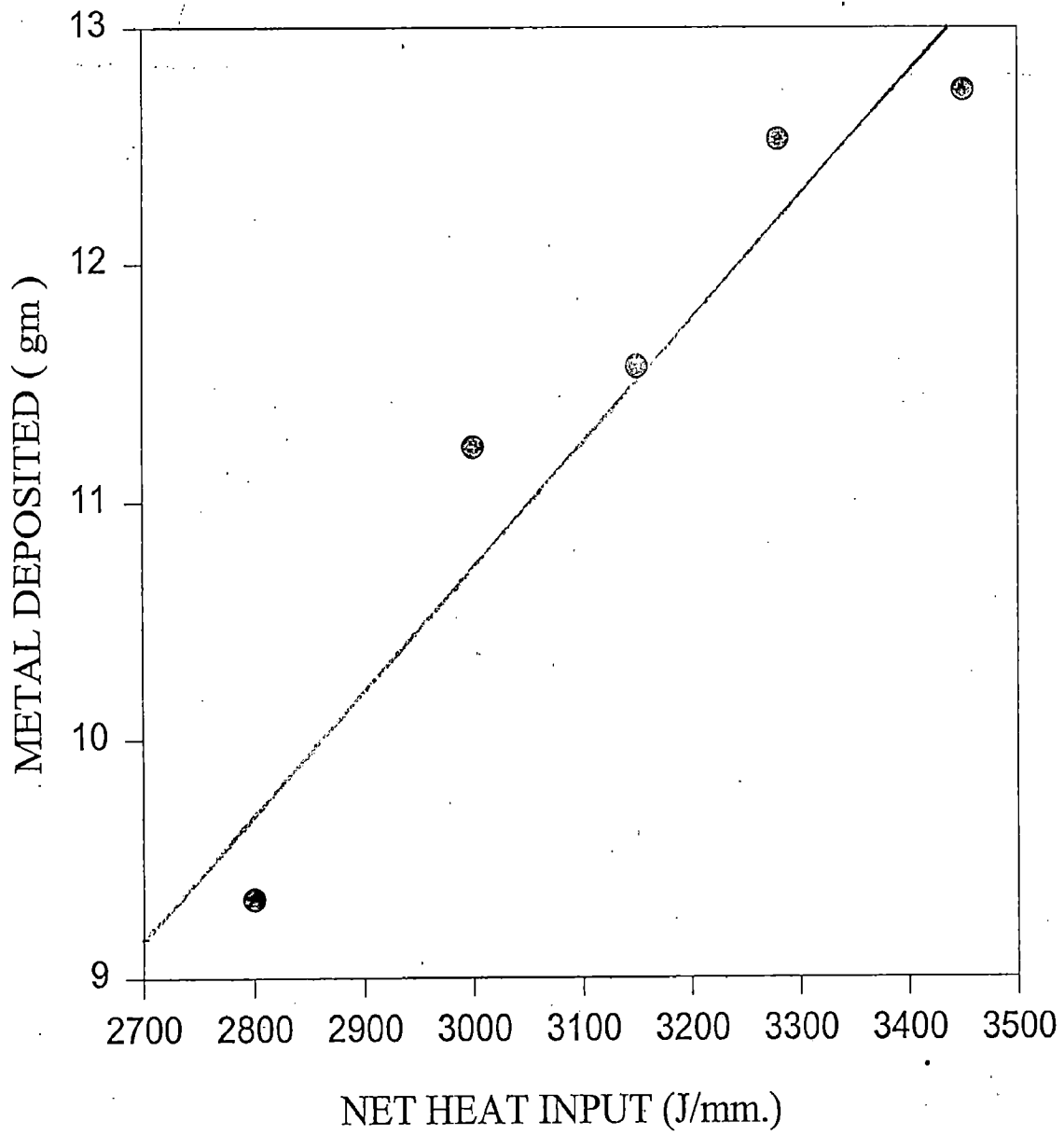


Fig. 4.1 Variation of metal deposited with net heat input.

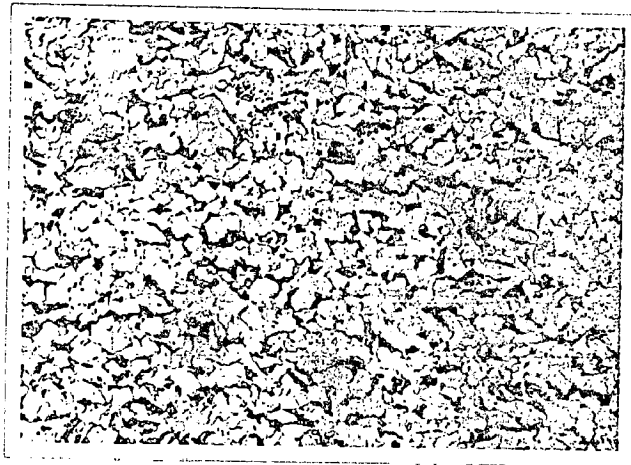


FIG.4.2 Optical micrograph of base metal ($\times 200$)

has been done by point counting technique. The average grain size of the ferrite phase is estimated to be 0.857μ . The grain size measurement has been done by intercept method. From the micrograph (Fig.4.2) it can be observed that ferrite grains are approximately polygonal and relatively smaller as compared to the grain size of the parent metal used by Siddique et al. [24]. This finer grain size in the steel presently used is attributed to the presence of Nb (0.02%). As one knows that Nb acts as a grain refiner.

4.2.2 Heat Affected Zone (HAZ)

The optical micrographs of HAZ of steel samples welded at heat input 2800 J/mm arc shown in Figs.4.3(a) & 4.3(b). Fig.4.3(a) shows the optical micrograph of the boundary region between base metal and HAZ. It can be clearly seen that the ferrite grains have recrystallized completely and some grain growth has taken place because the ferrite grains are bigger in size as compared to the ferrite grains in the base metal. Fig.4.3(b) shows the micrographs of the HAZ region where ferrite grains are even bigger in size and the second phase now appears in acicular (needle like) morphology. This may be a mixture of martensite and bainite.

The optical micrographs of HAZ at heat input 3000 J/mm are shown in Figs.4.4(a) & 4.4(b). Here one can also see recrystallized ferrite grains close to base metal and acicular structures towards the weld metal side (Fig.4.4(b)).

The optical micrographs of HAZ at heat input 3150 J/mm are shown in Figs.4.5(a) & 4.5(b). Similar type of observations can be made from these micrographs as compared to Fig.4.4(a) & Fig.4.4(b). However some lesser degree of acicularity can be observed in Fig.4.5(b).

The optical micrograph of HAZ at heat input 3280 J/mm is shown in Fig.4.6(a). It can be seen from the micrograph of HAZ that the extent of acicularity is even lesser than sample 4.5(b).

The optical micrograph of the HAZ of steel samples welded at heat input 3450 J/mm is shown in Fig.4.7(a). The ferrite grain size in this micrograph seems to be on the larger side as compared to the previous heat inputs. Some acicular microstructure is also visible.

These micrographs suggest that the temperature reached in the HAZ is between lower critical and solidus temperature line. Structure close to the fusion boundary shows larger grain growth as compared to the structure away from the fusion boundary. This is due to the fact that the temperature reached near the fusion boundary is much higher as compared to the temperature away from the fusion boundary. The presence of martensite along with pearlite can be attributed to the increased hardenability of the steel due to presence of Nb. The extent of formation of martensite has been found to be less in the work of Siddique et al. [24]. Because the steel used by Siddique et al. is plain C-steel of 6 mm thickness. In the optical micrographs one can distinguish martensite phase from pearlite as pearlite etches darker than martensite [25].

4.2.3 Weld Metal

The optical micrograph of the weld metal of the samples welded at heat input 2800 J/mm is shown in Fig.4.3(c). Here one can observe typical cast metal structure and widmanstatten structure. Dendrites of ferrites (white areas) can be clearly seen. Interdendritic regions which are black in the micrograph consist of pearlite-martensite mixture. Apart from this fine ferrite needles comprise widmanstatten structure.

The optical micrograph of the weld metal of the samples welded at heat input 3000 J/mm is shown in Fig.4.4(c). Here again one can observe a cast metal structure. However slightly coarser ferrite dendrites can be observed.

The optical micrograph of the weld metal of the samples welded at heat input 3150 J/mm is shown in Fig.4.5(c). Here once again one can observe the cast metal structure with dendrites of ferrite (white areas) and interdendritic regions of

pearlite and martensite.

The optical micrograph of the weld metal of the samples welded at heat input 3280 J/mm and 3450 J/mm are shown in Fig.4.6(b) & Fig.4.7(b) respectively. One observes coarser dendrites of ferrite in higher^{heat} input samples.

The optical micrographs in the weld metal region show typical cast structure. This is due to the fact that temperature reached in this region is well above the liquidus/temperature. The formation of the weld pool and its subsequent cooling makes the weldmetal region. It is further observed that as heat input increases the size of the weld pool increases. The bigger is the weld pool, the more the heat content of the weld pool. The bigger the weld pool or the higher the net heat input means slower the rate of cooling. The slower rate of cooling in higher net heat input rate is due to lesser temperature difference between the weld pool and adjoining areas. So grain coarsening has been observed in the weld metal region with increased heat inputs, [Figs.4.6(b) & 4.7(b)]. The extent of grain coarsening in the weldmetal region in the present work is of the same order as compared to the work of Siddique et al. [24].

4.3 HARDNESS PROFILE

The variation of macrohardness (VHN) with distance from weld centre of the welded specimens for heat inputs 2800, 3000, 3150, 3280, 3450 J/mm are shown in Figs.4.8 to 4.12 and data are given in Tables 4.2 to 4.6. It has been generally observed that hardness falls as one moves from weld centre towards base plate region. It is further observed that peak hardness values decrease with increasing net heat input. For example for Hnet 2800 J/mm the peak hardness value is 197 VHN whereas for the highest net heat input i.e. 3450 J/mm the peak hardness is only 179 VHN. Peak hardness values are 193, 187, 184 for net heat inputs 3000, 3150 and 3280 J/mm respectively. Hardness values also decreased in the HAZ with increase in net heat input. Hardness values are found to be 190, 188, 182, 180 and 177 VHN at a distance of 4.00 mm from weld centre for corresponding heat inputs 2800, 3000,

3150, 3280 and 3450 J/mm respectively. The decrease in hardness values with increase in net heat input is attributed to grain coarsening and slow rate of cooling encountered. As one knows with increase in net heat input the size of the weld pool increases and hence slower rate of cooling. Grain coarsening with increasing net heat input can be observed as shown in Figs.4.3(c), 4.4(c), 4.5(c), 4.6(b) and 4.7(b) for weld metal and in Figs.4.3(b), 4.4(b), 4.5(b), 4.6(a) and 4.7(a) for HAZ.

4.4 BEND TEST

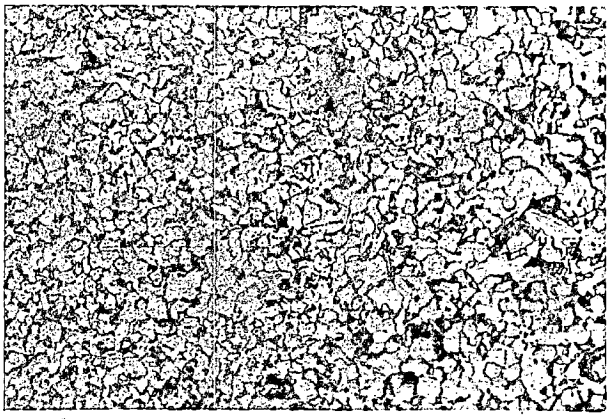
The photograph of the bend test samples are shown in Fig.4.13. The welded samples have been successfully bent in universal testing machine. The maximum bend angle obtained is 80° . No cracks have been observed in the weldment.

This suggests that there is sufficient ductility in these samples welded under the 2800 J/mm to 3450 J/mm heat inputs.

4.5 WIDTH OF WELDMENT

Different regions of a welded sample may clearly be seen after macroetching as shown in Fig.4.14. In present investigation we found that the width of weldment increases with increase in net heat input. It is shown in Fig.4.15.

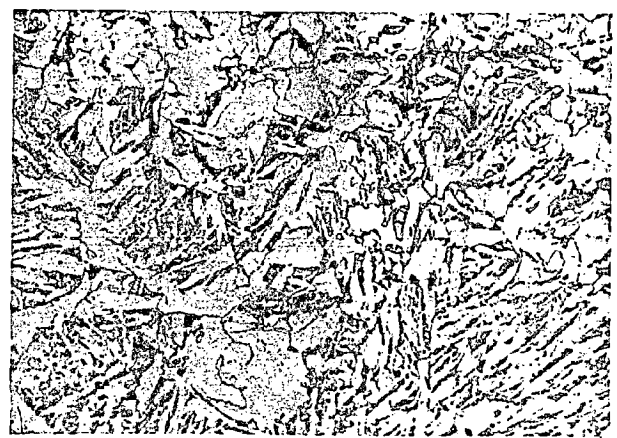
As we know that when the heat input is increased, the bigger weld pool will be formed that is the heat content will be more. Thus more area will be covered by higher temperature which leads to the increase in width of weldment. Thus it is clear that the width of weldment increases with increase in net heat input.



(a)



(b)



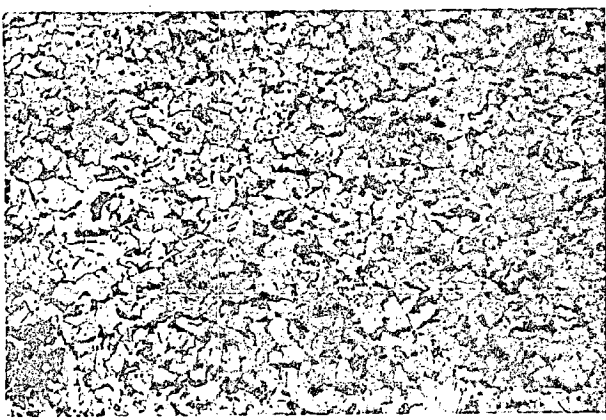
(c)

FIG. 4.3 Optical micrographs of HAZ and weldmetal for $H_{net}=2800 \text{ J/mm}$ ($\times 200$)

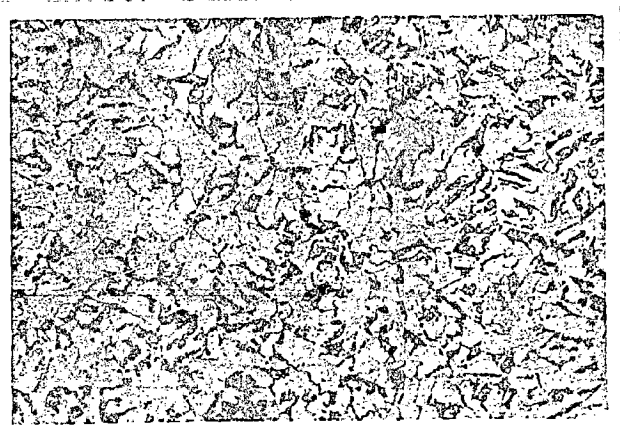
(a) Boundary region between base metal & HAZ.

(b) HAZ

(c) Weld metal



(a)



(b)

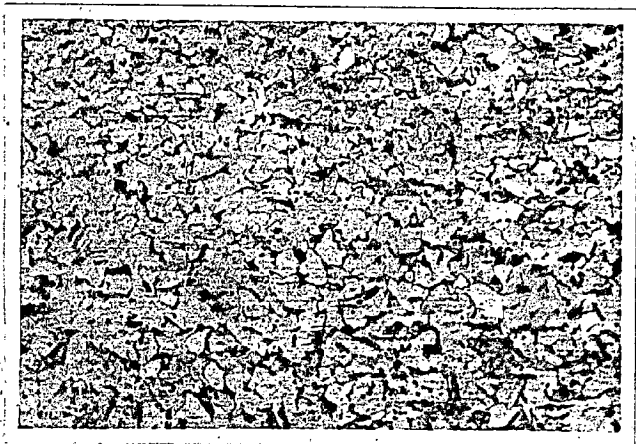


(c)

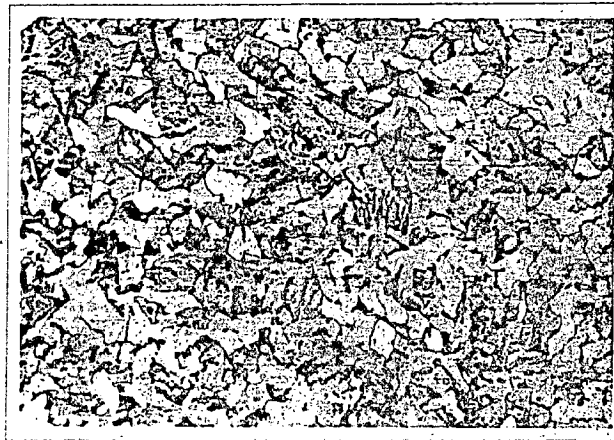
FIG.4.4 Optical micrographs of HAZ and weldmetal for $H_{net}=3000 \text{ J/mm}$ ($\times 200$)

(a) & (b) HAZ

(c) Weld metal



(a)



(b)



(c)

FIG. 4.5 Optical micrographs of HAZ and weldmetal for $H_{net}=3150 \text{ J/min}$ ($\times 200$)

(a) & (b) HAZ

(c) Weld metal



(a)



(b)

FIG.4.6 Optical micrographs of HAZ and weldmetal for $H_{net}=3280 \text{ J/mm}$ ($\times 200$)

(a) HAZ

(b) Weld metal



(a)



(b)

FIG. 4.7 Optical micrographs of HAZ and weld metal for $H_{net}=3450 \text{ J/mm}$ ($\times 200$)

(a) HAZ

(b) Weld metal

DISTANCE FROM WELD CENTRE (MM)	MACROHARDNESS (VHN)
0	197
2	193
4	190
5	187
6	182
9	173
10	166
12	163
13	161
14	160
16	160
18	160
20	160

**TABLE 4.2 MACROHARDNESS VS DISTANCE FROM
WELD CENTRE**

LOAD = 30 KG H NET = 2800 J/MM

DISTANCE FROM WELD CENTRE (MM)	MACROHARDNESS (VHN)
0	193
2	192
4	188
6	188
8	187
10	174
12	172
14	165
16	163
18	163
20	163
22	163

**TABLE 4.3 MACROHARDNESS VS DISTANCE FROM
WELD CENTRE**

LOAD = 30 KG H NET = 3000 J/MM

DISTANCE FROM WELD CENTRE (MM)	MACROHARDNESS (VHN)
0	187
2	184
4	182
6	172
8	166
11	164
13	164
15	165
17	165
20	165

**TABLE 4.4 MACROHARDNESS VS DISTANCE FROM
WELD CENTRE**

LOAD = 30 KG H NET = 3150 J/MM

DISTANCE FROM WELD CENTRE (MM)	MACROHARDNESS (VHN)
0	184
2	182
4	180
6	176
8	173
10	170
12	170
15	168
17	168
19	167
22	167
25	167

TABLE 4.5 MACROHARDNESS VS DISTANCE FROM
WELD CENTRE

LOAD = 30 KG

H NET = 3280 J/MM

248024



DISTANCE FROM WELD CENTRE (MM)	MACROHARDNESS (VHN)
0	179
2	179
4	177
6	176
8	176
10	175
12	172
14	170
16	169
19	169
21	169
23	169
25	169

**TABLE 4.6 MACROHARDNESS VS DISTANCE FROM
WELD CENTRE
LOAD=30 KG H NET =3450 J/MM**

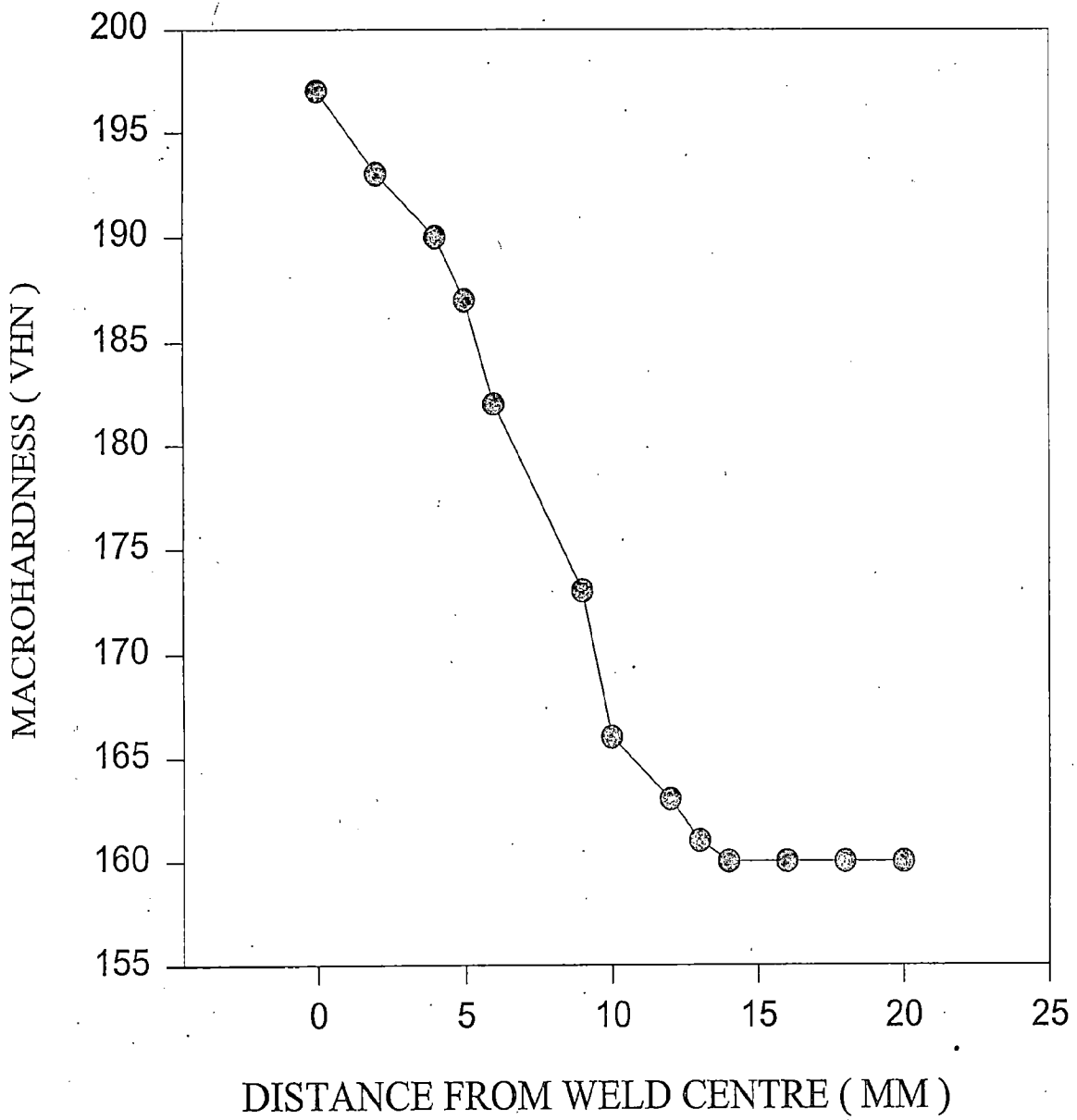


FIG. 4.8. Variation of macro hardness with distance from weld centre for $H_{net} = 2800 \text{ J/mm}$.

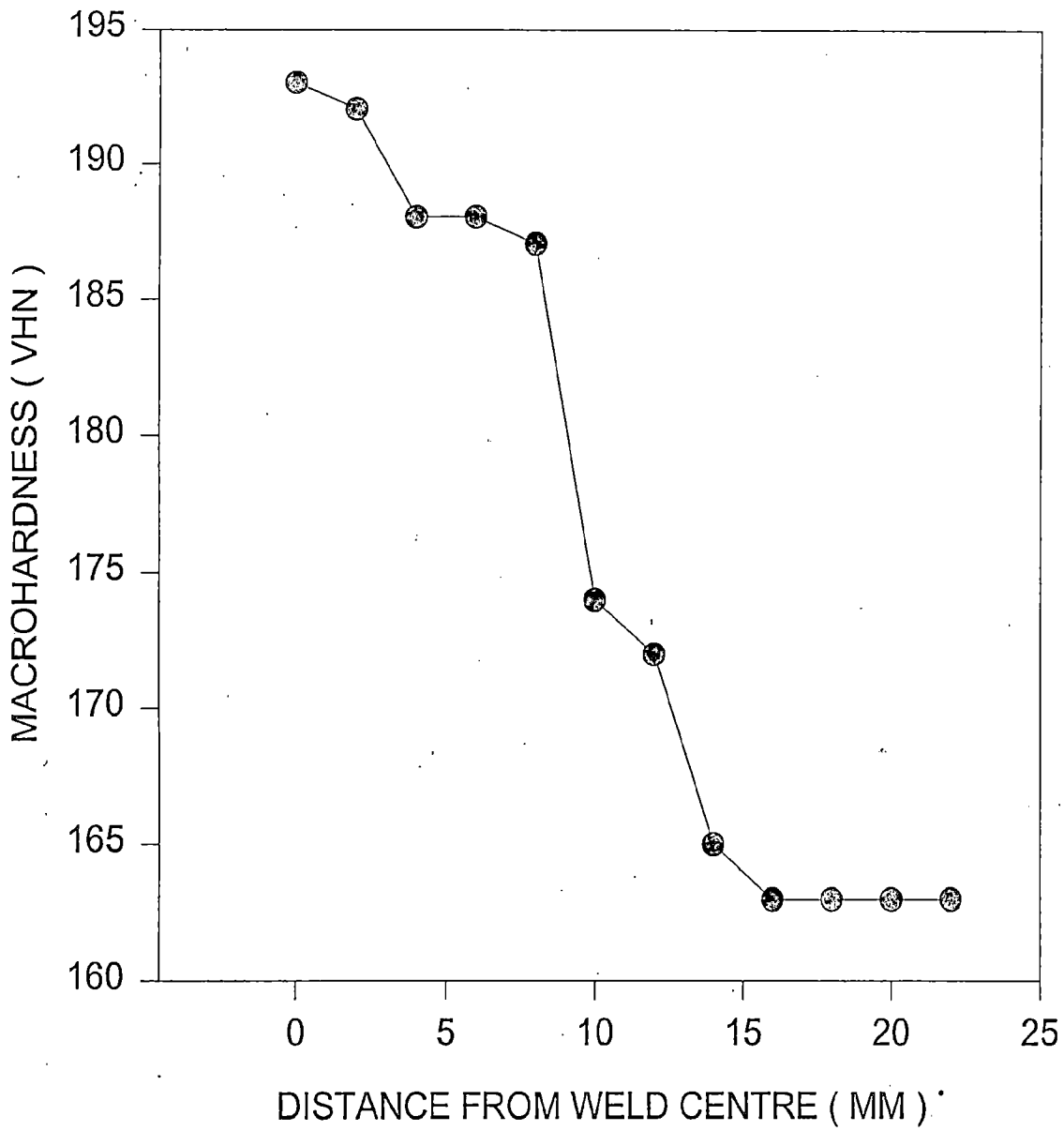


Fig. 4.9 Variation of macrohardness with distance from weld centre for $H_{net} = 3000 \text{ J/mm}$.

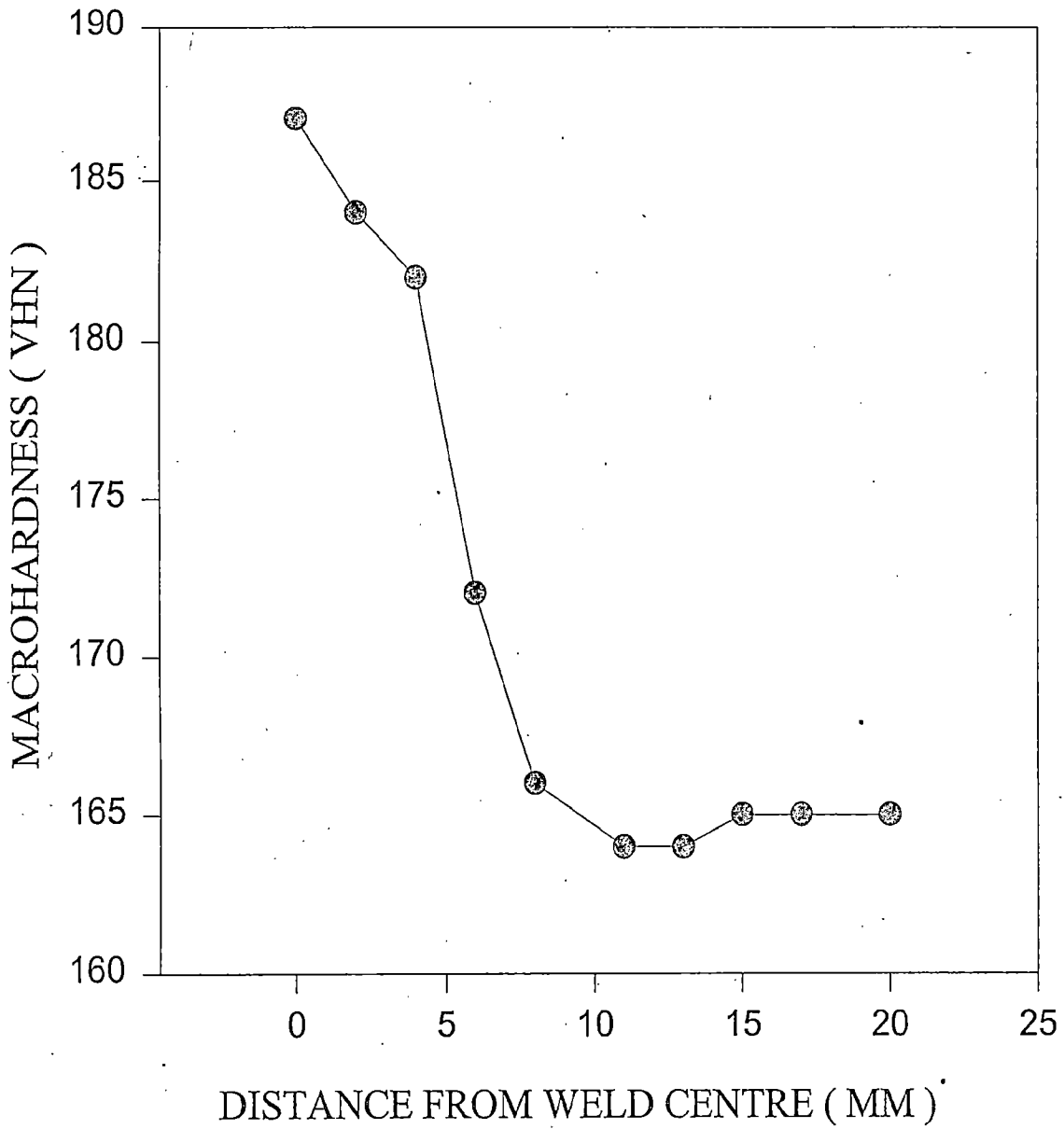


Fig. 4.10 Variation of macrohardness with distance from weld centre for $H_{net} = 3150 \text{ J/mm}$.

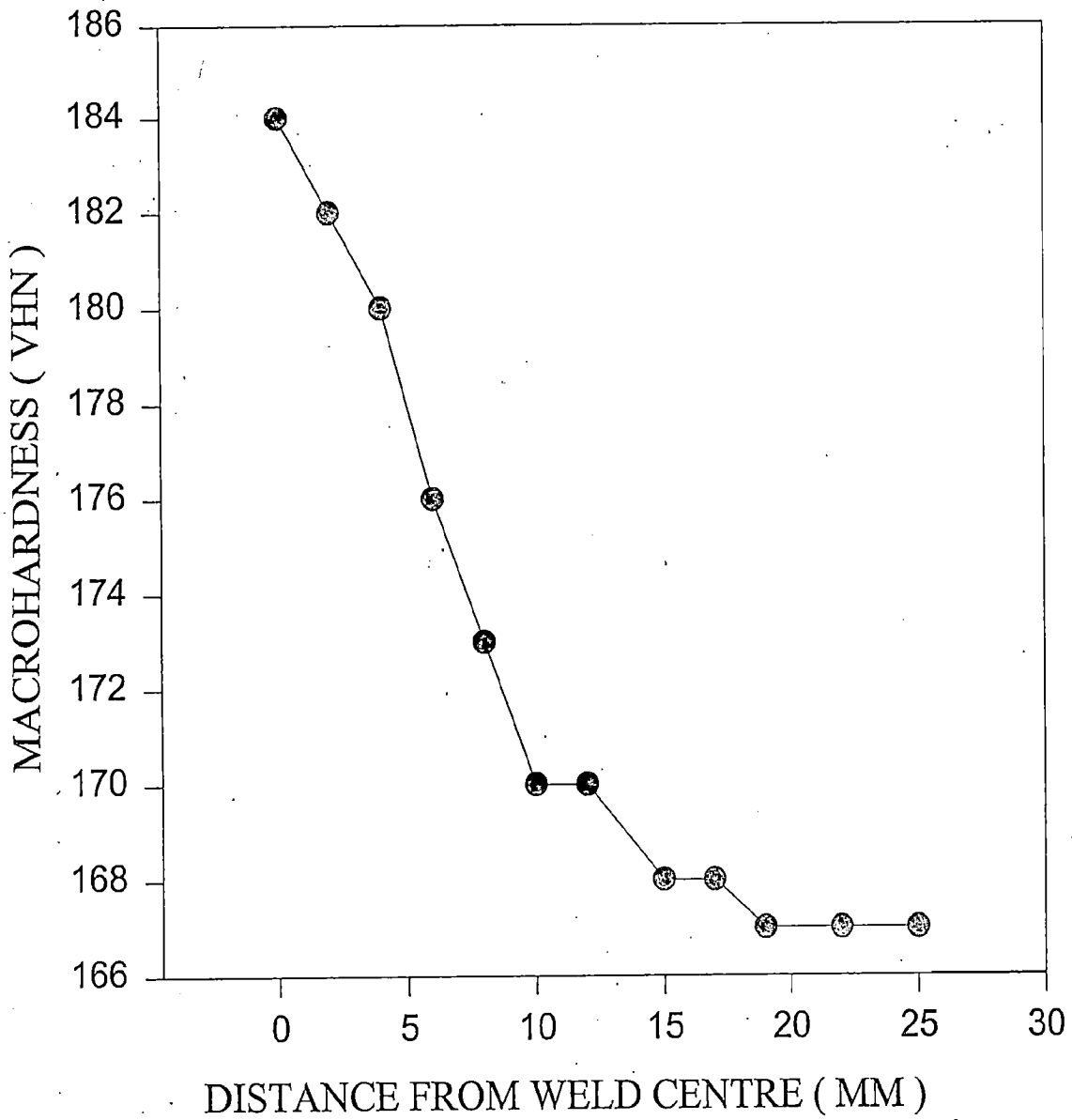


Fig. 4.11 Variation of macrohardness with distance from weld centre for $H_{net} = 3280 \text{ J/mm}$.

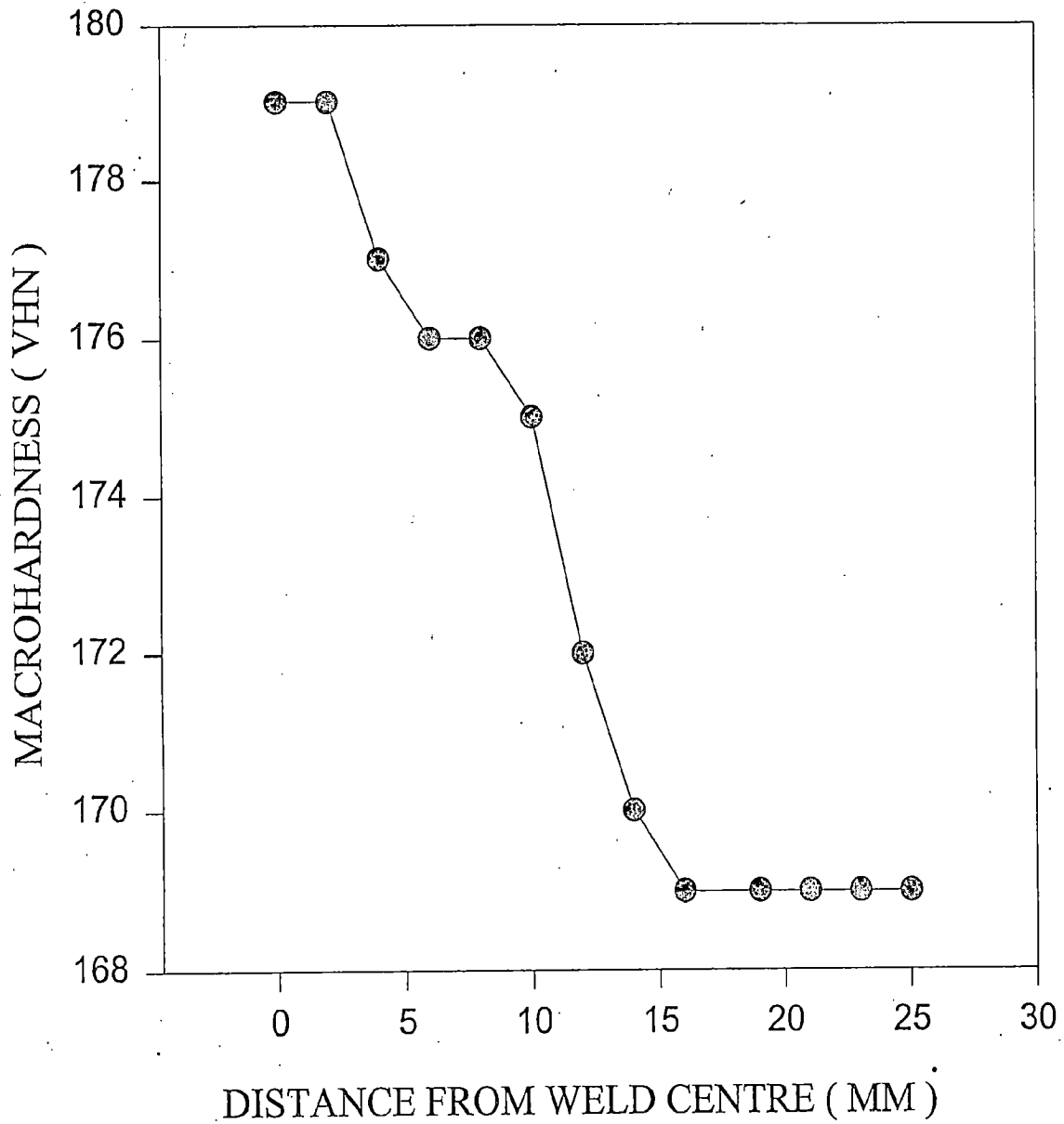


Fig. 4.12 Variation of macrohardness with distance from weld centre for $H_{net} = 3450 \text{ J/mm}$.

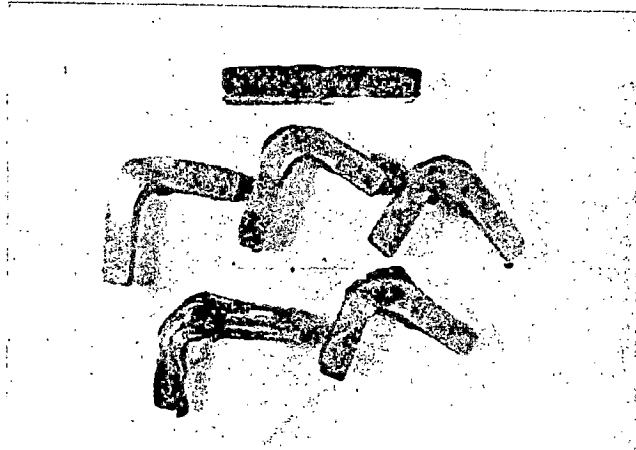


FIG. 4.13 Photograph of samples before and after bend test

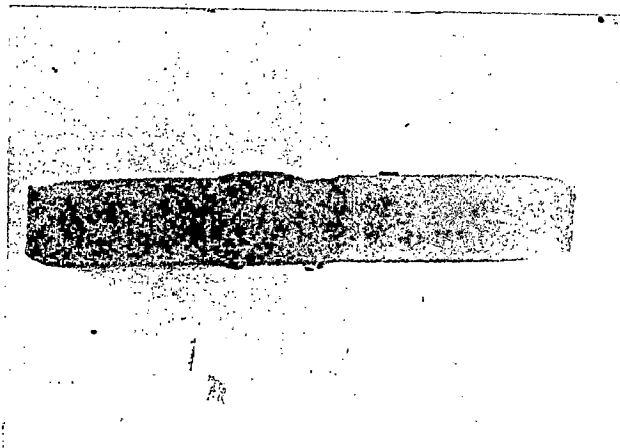


FIG. 4.14 Photograph of different zones seen in welded sample after macroetching

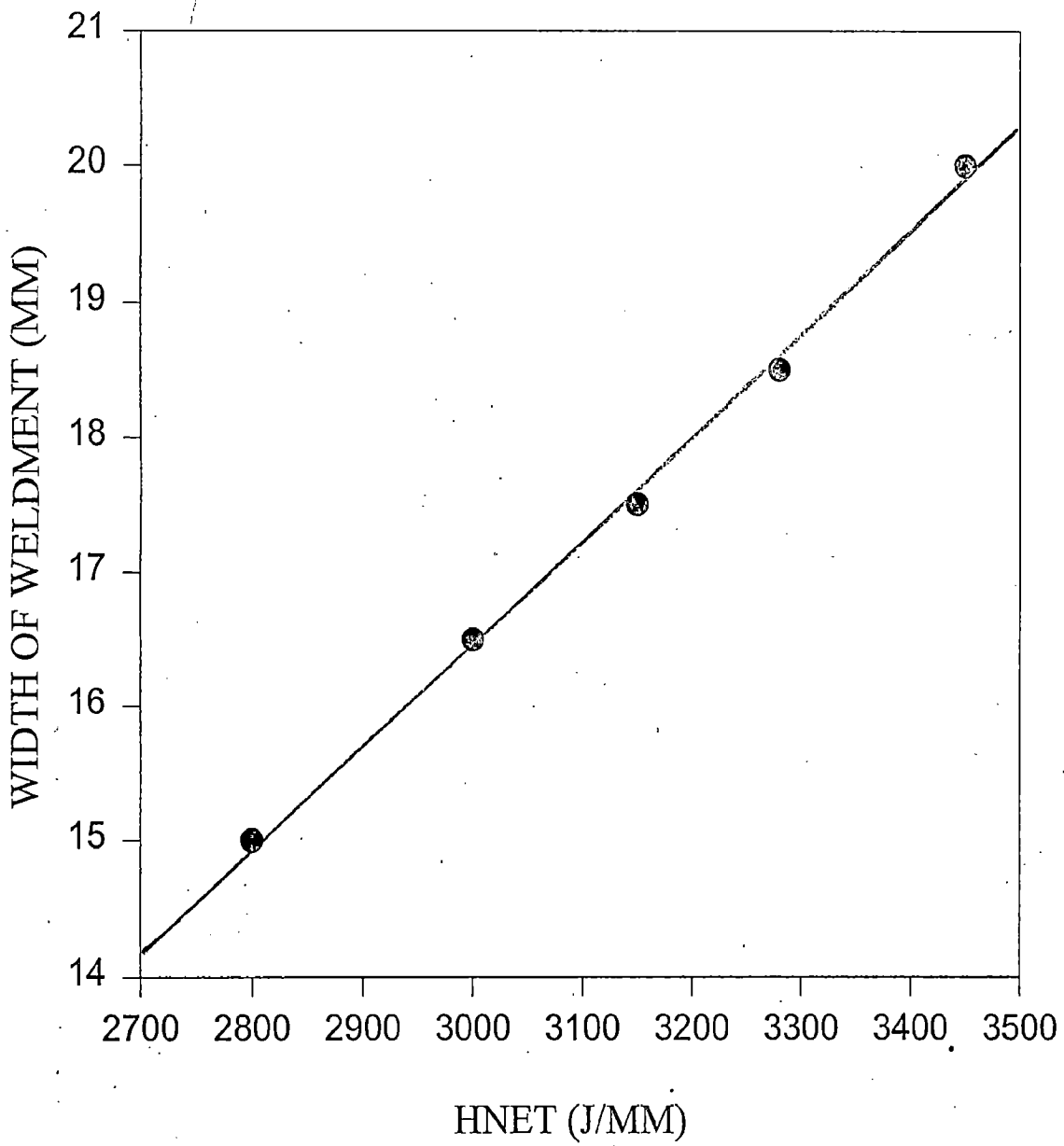


FIG 4.15 - Variation of weldment width with net heat input

CONCLUSIONS

The following conclusions can be drawn from the present work :

1. Metal deposition increases with increasing net heat input.
2. With increase in net heat input the hardness of weld metal decreases.
3. Maximum hardness has been obtained in the weldmetal region in all the samples irrespective of the heat input. This is attributed to presence of dendritic ferrite and acicular structures.
4. Hardness in the HAZ region close to the fusion boundary is found to be higher than hardness in the HAZ region close to the base metal irrespective of heat input.
5. In the region where the temperature in the metal plate is between A_1 and A_3 flowery pearlite has been found.
6. Coarser ferrite dendrites have been observed in the higher net heat input samples as compared to samples welded with lower net heat input.
7. Acicular microstructures have been observed in all the samples welded under different heat inputs.
8. No samples developed cracks during the bend test.

SUGGESTIONS FOR FUTURE WORK

The current investigation has highlighted several aspects. In light of these aspects few suggestions are being outlined below for future studies.

1. The same work may be carried out on same steel plate having more thickness and using submerged-arc welding process or any other welding process which is generally being used for these steels in industries.
2. The similar work may be carried out by using wider/different net heat input range.
3. Other mechanical tests such as tensile test, impact test may also be carried out in a similar work.
4. This study may be carried out on other steels also.

REFERENCES

1. Cornu, Jean, "Advanced Welding Systems", Vol. 1, pp. 12.
2. Tanaka, Tomo, "Overview of High Strength Steel", Transaction of Indian Institute of Metals, 49(3), June 1996, pp. 101-112.
3. Hrivnak, I., "The Mutual Relationship and Interdependence of Developments in Steel Metallurgy and Welding Technology", Welding in World, 16.1.1978.
4. Easterling, K.E., "Introduction to Physical Metallurgy of Welding", Butterworth and Company, London, England, 1983.
5. Zaczek, Z. and Cwiek, J., "Prediction of HAZ Hardness in Welds of Quenched and tempered HSLA Steels", Welding Journal, Jan. 1993, pp. 37s-40s.
6. Collins, L.E., Goddens, M.J. and Boyd, J.D., "Microstructure in Line Pipe Steels", Canadian Metallurgical Quarterly, 22(2), 1983, pp. 169-179.
7. Batra, N.K., Gupta, S.P., Shetty, M.N. and Tandon, R., Lecture Notes on Advances in Joining Processes, short term course, May 23-28, 1994.
8. Rosenthal, D., Welding Journal, 20(5), 1941, pp. 229s-234s.
9. Hart, P.H.M. and Harrison, P.L., "Compositional parameters for HAZ Cracking and Hardening in C-Mn Steels", Welding Journal, Oct. 1987, pp. 310s-322s.
10. Hunt, A.C., Kluken, A.O. and Edwards, G.R., "Heat Input and Dilution Effects in Microalloyed Steel Weld Metals", Welding Journal, Jan. 1994, pp. 9s-15s.
11. Goldak, J., Bibby, M., Moore, J. and Patel, B., Met. Trans., 17B, 1986, pp. 587-600.
12. Hougardy, H.P., "A Handbook of Materials Research and Engineering", Vol. 1, Springer-Verlag, Berlin, 1992, pp. 504-534.
13. Fairchild, D.P., Banguru, N.V. Koo, J.Y., Harrison, L.P. and Ozekcina, Welding Journal, 70(12), 1991, pp. 321s-329s.

14. Harrison, P.L. and Farrar, R.A., "Int. Materials Research", 34(1), 1989, pp. 35-51.
15. Brownrigg, M.J. and Boelen, K.M., "International Conference on HSLA Steel Technology and Applications", ASTM, Philadelphia, USA, 1984.
16. Khanna, O.P., "Welding Technology", Dhanpat Rai and Sons, Delhi, 1993.
17. Gianetto, J.A., Smith, N.J., McGrath, T. and Bowker, J.T., "Effect of Composition and Energy Input on Structure and Properties of High Strength Metals", Welding Journal, Vol. 71, No. 11, 1992.
18. Inagaki, M. and Sakiguchi, H., Trans of National Research Institute of Metals (Japan), 2:2, 1960, pp. 102-125.
19. "Welding Handbook", Seventh Ed., Vol. 4, American Welding Society, p. 2.
20. "Welding of HSLA (Microalloyed) structural Steel", American Society for Metals, 1976, pp. 1-5.
21. Cary, H.B., "Modern Welding Processes, 1985, pp. 179-180.
22. Poli, A., Santafe, C., Pozze, A. and Bertuzzi, L., "Effect of Flux and Chemical Composition on Mechanical Properties of Weld Metal in SAW", International Conference on Welding of Microalloyed Steel, 1976, p. 170.
23. Bernard, G., Faire, F., "Properties of Welds in SAW", International Conference on Welding of Microalloyed Steel, 1976, pp. 206-209.
24. Siddique, M.S., Nath, S.K. and Kaushal, G.C., "Microstructural Changes During Manual Metal Arc Welding of Plain Carbon Steel", Proc. IX ISME conference on Mechanical Engineering, No. 10-11, 1994, pp. 855-859.
25. Reed-Hill, Robert E., "Physical Metallurgy Principles", PWS Publishing Co., Boston, 1994, pp. 632-635.